

博士論文

Roles of 5-HT receptors in the morphological changes of
dendritic growth cones of rat cortical neurons *in vitro*
with special reference to cytoskeletons

平成26年度

筑波大学大学院人間総合科学研究科感性認知脳科学専攻

大谷 彰子

筑波大学

CONTENTS

ABSTRACT	4
INTRODUCTION	6
Development of the cerebral cortex	6
Development of cerebral cortical neurons <i>in vitro</i>	7
Serotonin neurons	7
5-HT receptors	9
Roles of 5-HT and 5-HT receptors in the development of the cerebral cortex.....	10
Neuronal cytoskeletons	11
Purpose of the present study	12
MATERIALS AND METHODS	14
Dissociated culture of cortical neurons.....	14
Immunocytochemistry of cytoskeletons and 5-HT receptors	15
Analysis of the dendrite formation	16
Analysis of the dendritic growth cone and protrusion morphology	17
Analysis of cytoskeletons in dendritic growth cone periphery	18
Time-lapse analysis	19
DiI-labeled dendritic growth cone <i>in vivo</i>	20
Statistical analysis	21
RESULTS	22
The distribution of cytoskeletons in dendrites	22
Expression of 5-HT1A and 5-HT2A receptors	22
Effects of 5-HT1A and 5-HT2A/2C receptor agonists on the dendrite formation	23
Effects of 5-HT1A and 5-HT2A/2C receptor agonists on dendritic growth cone periphery and protrusions	24

Effects of 5-HT _{2A/2C} receptor agonist on the MT dynamics and the actin depolymerization in dendritic growth cone periphery	25
Effects of 5-HT _{2A/2C} receptor agonist on the dynamic change of the dendritic growth cone morphology	26
The dendritic growth cone morphology <i>in vivo</i>	26
DISCUSSION	28
The type of cultured neurons	28
Effects of 5-HT receptors on dendritic growth cone periphery	28
The regulation of cytoskeletal proteins by 5-HT _{2A} receptor	30
Effects of 5-HT and 5-HT receptors on the dendrite formation	32
Roles of the dendritic growth cone dynamics <i>in vivo</i>	33
CONCLUSION	35
ACKNOWLEDGMENTS	36
REFERENCES	37

FIGURES and Table

Figure 1. Histogenesis of the cerebral cortex	
Figure 2. Architecture of microtubules	
Figure 3. Analysis of the dendrite formation	
Figure 4. Analysis of dendritic periphery and protrusions	
Table 1	
Figure 5. The experimental paradigm for the time-lapse analysis	
Figure 6. Cytoskeletal proteins in dendrites	
Figure 7. The expression of 5-HT _{1A} and 5-HT _{2A} receptors	
Figure 8. Effects of 8-OH DPAT, DOI and 5-HT on the dendrite formation	
Figure 9. Effects of 8-OH DPAT and DOI on dendritic growth cone periphery and protrusions	
Figure 10. Effects of 5-HT on dendritic growth cone periphery and protrusions	

Figure 11. Effects of DOI and 5-HT on cytoskeletal proteins in dendritic growth cone periphery

Figure 12. Effects of DOI on the expression of G-actin in dendritic growth cone periphery

Figure 13. Effects of DOI on the dynamics of the dendritic growth cone morphology

Figure 14. Dendritic growth cones of pyramidal neurons *in vitro*

ABSTRACT

Serotonin (5-HT) is involved in various aspects of the development of the cerebral cortex, but 5-HT receptors mediating effects of 5-HT are poorly understood. I investigated roles of serotonin 1A (5-HT_{1A}) and serotonin 2A (5-HT_{2A}) receptors in the dendrite development using the dissociation culture of the cerebral cortex of rat embryos. Neurons at embryonic day 16 were cultured for 4 days and then treated acutely with 5-HT_{1A} receptor agonist (8-OH DPAT), 5-HT_{2A/2C} receptor agonist (DOI) and 5-HT for 4 or 24 hours. 8-OH DPAT decreased the number of primary dendrites by both 4 and 24 hour-treatment. In contrast, DOI showed differential effects on the dendrite formation depending on the duration of the treatment, inhibiting the dendrite formation by 4 hour-treatment and promoting it by 24 hour-treatment. 5-HT had effects opposite to those of DOI. Next, I divided actin-rich structures into three types, growth cone periphery, dendritic shaft protrusions and somatic protrusions, and examined effects of the 5-HT receptor agonists and 5-HT on the size of growth cone periphery, the density of dendritic shaft protrusions and the number of somatic protrusions. 8-OH DPAT decreased the length of growth cone periphery, while DOI increased the length, width and area of growth cone periphery. The DOI-induced increase of the length may be mediated by 5-HT_{2A} receptor, because 5-HT_{2A} antagonist reversed the effects of DOI. 5-HT showed the similar effects to those of DOI on growth cone periphery. Furthermore, I examined effects of DOI on dendritic growth cone periphery with special reference to cytoskeletal proteins, tyrosinated α -tubulin (Tyr-T; dynamic tubulin), acetylated α -tubulin (Ace-T; stable tubulin) and globular actin (G-actin; depolymerized actin). DOI increased the mean fluorescence intensity of

Tyr-T, whereas decreased that of Ace-T in dendritic growth cone periphery. These effects were reversed by the 5-HT_{2A} receptor antagonist, suggesting that 5-HT_{2A} receptor may induce microtubule dynamics. DOI also increased the mean fluorescence intensity of G-actin, suggesting that DOI promotes the actin depolymerization. Finally, the time-lapse analysis demonstrated the increase of the morphological dynamics in dendritic growth cones by DOI treatment. The present study suggests that 5-HT_{1A} receptor inhibits the dendrite initiation, whereas 5-HT_{2A} receptor induces the morphological changes of dendritic growth cones and increased their dynamics. These effects on the dendritic growth cone morphology and dynamics may be mediated by the regulation of cytoskeletal proteins.

INTRODUCTION

Development of the cerebral cortex

The mammalian cerebral cortex is six-layered structure that contains both pyramidal and non-pyramidal neurons (Parnavelas, 2000; Molyneaux et al., 2007). Neuronal progenitors of the cerebral cortex proliferate in the ventricular zone (VZ) of the lateral ventricles. In rats, the first postmitotic neurons migrate from the VZ to form the preplate (PP) on embryonic day (E) 13 and E14 (Fig. 1). After E14, the subventricular zone (SVZ) appears outside the VZ and contains proliferating cells which give rise to both neurons and glia. Subsequently, the PP splits into the marginal zone (MZ; prospective layer I) at the pial surface and the subplate (SP) below accumulating neurons of the cortical plate (CP) after E16. At this stage, the intermediate zone (IZ) appears between the SP and SVZ and consists of tangentially oriented fibers (Bayer and Altman, 1990; Nadarajah and Parnavelas, 2002; Kriegstein et al., 2006). In the CP, early generating neurons reside in its deeper layer and late generating neurons in its superficial layer. Thus, neurons in layers VI, V, IV and II-III differentiate on E15-16, E16-17, E17-18 and E18-19, respectively. The cortical neurogenesis completes by E21-22, and the layer structure becomes similar to adult one by postnatal day (P) 6 (Lund and Mustari, 1977; Altman and Bayer, 1990; Ignacio et al., 1995; Kriegstein et al., 2006).

Axonal projections of the cortical neurons are different among the layers. Small- and medium-sized pyramidal neurons in layers II/III, V and VI project through the corpus callosum to the contralateral hemisphere. Large pyramidal neurons in layer V extend axons subcortically to the brainstem and spinal cord, and neurons in layer VI project to

the thalamus (O'Leary and Koester, 1993; Molyneaux et al., 2007). In layer IV, thalamocortical axons terminate densely (O'Leary and Koester, 1993)

Development of cerebral cortical neurons *in vitro*

In dissociated culture of the rat embryonic cerebral cortex, neurons begin to extend several neurites from the soma by 1 day *in vitro* (DIV). On 2DIV, a longer neurite appears among neurites. A single longer neurite and several shorter neurites differentiate into an axon and dendrites, respectively by 4DIV, and most neurons have dendritic branches by 7DIV. Thereafter, dendritic spines are formed on dendritic shafts between 7 and 21DIV, and the synapse formation occurs (De Lima et al., 1997; Hayashi et al., 2010; Harigai et al., 2011). The formation of dendritic branches and spines begins with dendritic filopodia which are protrusions from dendritic shafts. Dendritic filopodia act as precursors and extend to form branches or stabilize spine morphology (Hering and Sheng, 2001; Scott and Lou, 2001). Dendritic spines are mainly categorized into protrusions with a thin neck and a bulbous head (mushroom shaped) and protrusions without neck (puncta), and change into mushroom shaped structure from dendritic filopodia through puncta for matured synaptic function (Matus, 2005; Sekino et al., 2007; Gandou et al., 2010; Harigai et al., 2011; Yoshida et al., 2011).

Serotonin neurons

Serotonin (5-hydroxytryptamine, 5-HT) is one of the monoamines and acts as a neurotransmitter in the matured brain (Bockaert et al., 2006; Daubert and Condron 2010). 5-HT neurons are generated early during the development and 5-HT is released from the 5-HT neurons before synapses are established (Gasper et al., 2003). In the rat brain, 5-HT neurons differentiate on E11-12, and projections from the rostral raphe nuclei ascend to the midbrain and forebrain, whereas projections from the caudal raphe nuclei descend to the spinal cord (Rubenstein, 1998). Ascending projections begin to be detected on E12 and reach the mesencephalic flexure by E13-14 (Aitken and Tork, 1988; Lauder, 1990; Vitalis and Parnavelas, 2003). Then, the ascending projections divide into dorsal and ventral directions. By E15, a few 5-HT fibers turn dorsally and enter the fasciculus retroflexus, and many fibers course between the mammillary complex and the ventral thalamic area through the medial forebrain bundle (MFB) in the caudal diencephalon. The latter fibers spread out in both medial and lateral directions within the MFB and further ascend through the lateral hypothalamus. On E16-17, the most medial fibers extend rostrally from the lateral hypothalamus through the preoptic region, the septum and diagonal band of Broca, whereas the lateral fibers enter the lateral telencephalon penetrating the ganglionic eminence (GE). The majority of the medial fibers enters the cortex medially by E18 and lies in discrete layers above and below the CP, specifically in the MZ and IZ. On E19, these projections extend into lateral cortical fields through the entire surface of the frontal pole of the cortex. Some medial fibers appear to reach the hippocampus from the septum via fornix, and the lateral fibers enter the lateral cortex by passing ventral to the internal capsule through the GE. 5-HT fibers reach most of the telencephalon on E21, and the innervation pattern of 5-HT neuron in the cortex show similar to that in the adult cortex by P21 (Lidov and

Molliver, 1982a, 1982b; Lauder, 1990; Vitalis and Parnavelas, 2003).

5-HT receptors

5-HT receptors are classified into 7 families and at least 14 different subtypes have been identified; 5-HT1 (1A, 1B, 1D, 1E, 1F), 5-HT2 (2A, 2B, 2C), 5-HT3, 5-HT4, 5-HT5 (5A, 5B), 5-HT6 and 5-HT7 receptors (Barnes and Sharp, 1999; Bockaert et al., 2006; Celada et al., 2013). 5-HT3 receptor is only ligand-gated ion channel, and others are G-protein-coupled receptors with seven transmembrane domains (Celada et al., 2013). 5-HT1 receptors and 5-HT2 receptors are coupled to $G\alpha_i/G\alpha_o$ and $G\alpha_q$ proteins, respectively, whereas 5-HT4, 5-HT6 and 5-HT7 receptors are coupled to $G\alpha_s$ proteins. G-proteins to which 5-HT5 receptor is coupled have not been revealed completely. It was reported that 5-HT5A receptor is coupled to $G\alpha_i/G\alpha_o$, but G-protein coupling to 5-HT5B receptor is still uncertain (Bockaert et al., 2006; Filip and Bader, 2009; Pytliak et al., 2011).

In the adult cerebral cortex, 5-HT receptors, particularly 5-HT1A and 5-HT2A receptors, are expressed most abundantly in the prefrontal cortex (PFC). In the rat PFC, 50% of pyramidal neurons and 20-30% of GABAergic interneurons express the mRNA of 5-HT1A or 5-HT2A receptor, and around 80% of these neurons co-express the mRNAs of both receptors (Amargos-Bosch et al., 2004). Other 5-HT1 receptor subtypes, 5-HT1B, 5-HT1D, 5-HT1E and 5-HT1F receptors are also present in the cortex. Among these receptors, 5-HT1B and 5-HT1E receptors are highly expressed in the frontal cortex (Lanfumeey and Hamon, 2004; Filip and Bader, 2009). In addition to 5-HT2A

receptor, 5-HT_{2C} receptor is highly expressed in the brain, although the expression of 5-HT_{2B} receptor is very low. 5-HT_{2C} receptor is expressed richly in pyramidal neurons of the PFC, but the degree of co-expression with 5-HT_{1A} and 5-HT_{2A} receptors is unknown. 5-HT₃ receptor is present in the cortex and is localized in GABAergic interneurons. 5-HT₄ receptor is expressed weakly in the cortex, but the single-cell RT-PCR revealed that up to 60% of pyramidal neurons in the PFC contain 5-HT₄ receptor mRNA. In 5-HT₅ receptor family, 5-HT_{5B} receptor mRNA is highly present in the cortex, while 5-HT_{5A} receptor mRNA is absent. 5-HT₆ receptor mRNA is more abundant in the hypothalamus, hippocampus and striatum relative to the cortex. 5-HT₇ receptor is mainly distributed in the thalamus, hypothalamus, hippocampus and amygdala in addition to the cortex (Bockaert et al., 2006; Flip and Bader, 2009; Victoria Puig and Gullledge, 2011; Celada et al., 2013).

Roles of 5-HT and 5-HT receptors in the development of the cerebral cortex

Axonal projections of 5-HT neurons start from early embryonic stages as described above, which suggests that 5-HT has crucial roles in the neural development (Gaspar et al., 2003; Oostland and Fooft, 2013). There are some studies which show roles of 5-HT in the development of the cerebral cortex. In rats, 5-HT promotes the survival and differentiation of excitatory neurons (Dooley et al., 1997; Lavdas et al., 1997), inhibits the branching of neurites (Sikich et al., 1990) and promotes the synapse formation (Chubakov et al., 1986; Matsukawa et al., 2003). Additionally, the administration of 5-HT synthesis inhibitor to embryos inhibits the dendrite elongation and branching of

pyramidal neurons in the adult cerebral cortex (Vitalis et al., 2007).

In contrast, roles of 5-HT receptors mediating these actions in the development of the cerebral cortex are not well understood. 5-HT_{1A} receptor inhibits the neurite branching (Sikich et al., 1990) and the maturation of dendritic spines (Yoshida et al., 2011). 5-HT_{2A/2C} receptor agonist promotes the spine formation (Jones et al., 2009; Yoshida et al., 2011). 5-HT₃ receptor inhibits the formation of dendrites (Hayashi et al., 2010), whereas 5-HT₇ receptor promotes the neurite outgrowth (Speranza et al., 2013). Among these 5-HT receptors, 5-HT_{1A} and 5-HT_{2A} receptors appear early in the developing brain. 5-HT_{1A} receptor is expressed from E12 in the rat brain, and 5-HT_{2A} receptor is expressed from E18 in the rat cerebral cortex and this expression level increases as the development progresses (Hellendall et al., 1993; Hillion et al., 1993, 1994; Li et al., 2004). Although there are some reports about the roles of 5-HT_{1A} and 5-HT_{2A} receptors in the neurite and spine formation as shown above, roles of these receptors in the early stages of the dendrite formation are not clear.

Neuronal cytoskeletons

Major cytoskeletons in dendrites and axons are actin and microtubules (MTs). In addition, microtubule-associated proteins (MAPs) bind to MTs and regulate the polymerization and stabilization of MTs or cross-linking of filamentous actin (F-actin) and MTs (Sanchez et al., 2000; Dehmelt and Halpain, 2004; Georges et al., 2008; Poulain and Sobel, 2010). Actin and MTs play important roles in the neurite outgrowth. In the axonal outgrowth, changes in the direction depend on the reorganization of actin

and MTs in growth cones (Lowery and Vactor, 2009). The polymerization of monomeric globular actin (G-actin) occurs at one end (barbed end) of F-actin and the depolymerization occurs at the opposite end (pointed end) (Mitchison and Kirschner, 1988). MTs consist of polymerized α -tubulin and β -tubulin and are the polar structures with the plus end and the minus end, which are terminated by β -subunit and α -subunit, respectively (Baas et al., 1989; Howard and Hyman, 2003). Highly tyrosinated α -tubulin (Tyr-T) is rich in the plus end and highly acetylated α -tubulin (Ace-T) in the minus end (Fig. 2). The polymerization and depolymerization of MTs occur rapidly in the plus end, while the depolymerization occurs slowly in the minus end. Therefore, Tyr-T and Ace-T are known as index of dynamic MTs and stable MTs, respectively. Moreover, it was reported that the individual dynamic MTs run parallel to F-actin bundles in axonal growth cones and dynamic MTs may act as guidance sensors (Dent and Kalil 2001; Dent and Gertler, 2003; Conde and Caceres, 2009; Lowery and Vactor, 2009). It was also shown that MTs are present in dendritic spines, and dynamic MTs regulate the amounts of F-actin within spines and are necessary for the maintenance of spine morphology and the synaptic plasticity (Gu et al., 2008; Jaworski et al., 2009; Penzes et al., 2009). These results suggest that the dynamics of actin and MTs are important for the dendritic spine morphology and function. However, roles of actin and MTs in dendritic growth cones at early developmental stages remain to be examined.

Purpose of the present study

In the present study, I examined roles of 5-HT_{1A} and 5-HT_{2A} receptors in the dendrite

development with special reference to the morphological changes and/or dynamics of dendritic growth cones of cortical neurons *in vitro*. In addition, I examined the assembly of actin and MT as underlying mechanisms for actions of 5-HT_{2A} receptor in dendritic growth cones.

MATERIALS AND METHODS

All the experiments followed the Guide for the Care and Use of Laboratory Animals described by the National Institutes of Health (USA), and were approved by the Animal Experimentation Committee of University of Tsukuba.

Dissociated culture of cortical neurons

Wistar/ST strain rats (Nihon SLC, Hamamatsu, Japan) were used in the present study, and the day of the vaginal plug was considered to be E0. Embryos at E16 were removed from pregnant rats under the deep anesthesia by isoflurane (Mylan, Tokyo, Japan). Embryos were quickly decapitated and the cerebral cortex was excised. After the careful removal of meninges, the cerebral cortex was incubated in 0.05% trypsin-EDTA (Life Technologies, Carlsbad, CA) for 5 minutes at 37°C and cells were dissociated by trituration with a Pasteur pipette. After filtration with 70- μ m nylon cell strainer (BD Falcon, San Jose, CA), dissociated cells were plated on 8-well chamber slides (NUNK, Rochester, NY) coated with 0.2% polyethyleneimine (Sigma, St. Louis, MO) at a density of 4×10^4 cells/cm². The cells were cultured in Minimal Essential Medium (Life Technologies) supplemented with 10% heat-inactivated fetal bovine serum (Life Technologies), 0.5 mM L-glutamine (Life Technologies), 25 μ M glutamate (Wako, Osaka, Japan) and 25 μ g/ml penicillin/streptomycin (Sigma) in a humidified atmosphere of 95% air-5% CO₂ at 37°C. One day after plating, 5 μ M cytosine- β -arabino-furanoside (Ara-C; Sigma) was added for 24 hours in Neurobasal Medium (Life Technologies)

with 2% B-27 supplement (Life Technologies), 0.5 mM L-glutamine and 25 µg/ml penicillin/streptomycin to remove proliferating glial and neuronal progenitors. The Ara-C treatment has been shown to remove GFAP-positive glial cells (Hayashi et al., 2010).

Immunocytochemistry of cytoskeletons and 5-HT receptors

Cortical neurons were cultured for 4 days and fixed with 4% paraformaldehyde (PFA) in 0.1 M phosphate buffer (PB) for 30 minutes at room temperature. Nonspecific antibody binding was blocked by the incubation with 1% bovine serum albumin (only in case of 5-HT1A antibody) or 2% normal goat serum (NGS) and 0.1% Triton X-100 in 0.1 M PB for 30 minutes. To examine the distribution of cytoskeletons in dendrites, neurons were then incubated overnight at 4°C with chick anti-microtubule-associated protein 2 (MAP2) antibody (1:4000 dilution, Chemicon, Temecula, CA) and mouse anti-β-tubulin antibody (1:5000 dilution, Promega, Madison, WI). Neurons were then incubated with biotinylated goat anti-chick IgG antibody (1:500 dilution, Vector Laboratories, Burlingame, CA) and Alexa Fluor 488-conjugated goat anti-mouse IgG (1:500 dilution, Life Technologies) for 1 hour at room temperature. They were then incubated with streptavidin-conjugated Pacific Blue (1:500 dilution, Life Technologies) and rhodamine-phalloidin (1:100 dilution, Life Technologies) which selectively stains F-actin for 1 hour and 30 minutes at room temperature, respectively.

To examine the expression of 5-HT1A and 5-HT2A receptors, cultured neurons were incubated overnight at 4°C with the affinity-purified goat anti-5-HT1A receptor

antibody (1:100 dilution, Santa Cruz Biotechnology, Dallas, TX) or rabbit anti-5-HT_{2A} receptor antibody (1:1000 dilution) which was raised against the C-terminus of the 5-HT_{2A} receptor (Hamada et al., 1998). Immunostaining of the primary antibody which was adsorbed by the antigenic peptide or without the primary antibody yielded no specific staining (Hamada et al., 1998). I also confirmed specificity of the antibody in cultured neurons by immunostaining without the primary antibody. After the incubation with the 5-HT_{1A} or 5-HT_{2A} receptor antibody, cultured neurons were incubated with FITC-conjugated donkey anti-goat IgG antibody (1:500 dilution, Jackson ImmunoResearch Laboratories, West Grove, PA) or Alexa Fluor 488-conjugated goat anti-rabbit IgG antibody (1:500 dilution, Life Technologies) for 1 hour at room temperature, respectively. Neurons were then incubated with rhodamine-phalloidin for 30 minutes. X-Y or Z-stack images of stained neurons were taken respectively at 20x or 63x with a confocal laser-scanning microscope (LSM 510META ver.3.2, Carl Zeiss, Oberkochen, Germany).

Analysis of the dendrite formation

At 4 days in vitro (DIV), 5-HT_{1A} receptor agonist ((R)-(+)-8-hydroxy-2-di-n-propylamino-tetralin, 8-OH DPAT, Sigma), 5-HT_{2A/2C} receptor agonist ((±)-2,5-demethoxy-4-iodoamphetamine hydrochloride, DOI, Sigma) and 5-HT (Sigma) was added at the concentration of 1, 10 and 100 nM for 4 or 24 hours. The cultured neurons were fixed and incubated with NGS as described above. The neurons were then incubated overnight at 4°C with the MAP2 antibody and mouse anti-glutamate

decarboxylase 65/67 (GAD65/67) antibody (1:1000 dilution, Chemicon). They were then incubated with biotinylated goat anti-chick IgG antibody and Alexa Fluor 488-conjugated goat anti-mouse IgG for 1 hour at room temperature, and then incubated with streptavidin-conjugated Pacific Blue for 1 hour at room temperature. X-Y images of stained neurons were taken at 20x with the confocal laser scanning microscope. To examine the effects of 8-OH DPAT, DOI and 5-HT on the dendrite formation, the MAP2-positive longest neurite was excluded, because it was a putative axon (De Lima et al., 1997; Hayashi et al., 2010). Only GAD65/67-negative neurons were examined. The number of primary dendrites, average dendrite length (total dendrite length/number of primary dendrites) and branching index (total number of branch points/number of primary dendrites) were measured by an image analyzing software (Neurocyte Image Analyzer Ver. 1.5, Kurabo, Osaka, Japan) (Fig. 3; Hayashi et al., 2010; see also Gandou et al., 2010; Harigai et al., 2011; Li et al., 2012). The number of primary dendrites, average dendrite length and branching index indicate dendrite initiation, dendrite elongation and dendrite arborization, respectively. The numbers of neurons for the analysis of dendrites are shown in Table 1.

Analysis of the dendritic growth cone and protrusion morphology

At 4DIV, neurons were treated with 8-OH DPAT, DOI and 5-HT for 4 hours and immunostained by anti-MAP2 and anti-GAD65/67 antibodies as described above, followed by the incubation with rhodamine-phalloidin for 30 minutes at room temperature. To examine the specificity of the effect of DOI, 5-HT_{2A} receptor

antagonist (ketanserin, Tocris Bioscience, Bristol, UK) was added in combination with DOI at concentrations of 1000 nM. Z-stack images of stained neurons were taken at 63x with the confocal laser scanning microscope. To examine effects of each drug on the dendrite morphology, I examined three parameters of F-actin-positive and MAP2-negative structures. Thus I measured the length of “growth cone periphery” at the tip of dendritic growth cones, the number of “dendritic shaft protrusions” per unit dendrite length which are protrusions emerging directly from the dendritic shaft and the number of “somatic protrusions” per neuron which are protrusions emerging directly from the cell body (Fig. 4A). The length of growth cone periphery, the number of dendritic shaft protrusions, and the number of somatic protrusions may be related to the dendrite elongation, dendrite branching, and formation of primary dendrites, respectively. The width and area of growth cone periphery were also measured. The width index was determined by the ratio of head width (width of the most spread portion of F-actin-positive and MAP2-negative dendrite tip) and neck width (width of the thinnest portion) (Fig. 4B). The measurement of area was performed by ImageJ software. In this analysis, only GAD65/67-negative neurons were analyzed. The numbers of growth cones for the analysis of the length, width and area of growth cone periphery, the number of dendrites for the analysis of the density of the dendritic shaft protrusions, and the number of neurons for the analysis of the somatic protrusions are shown in Table 1.

Analysis of cytoskeletons in dendritic growth cone periphery

Neurons were cultured for 4 days and treated by DOI or 5-HT (1, 10, 100 nM) for 4 hours as described above. Neurons were immunostained by rat anti-tyrosinated α -tubulin (Tyr-T) antibody (clone YL1/2; 1:500 dilution, Chemicon) or mouse anti-acetylated α -tubulin (Ace-T) antibody (clone 6-11B-1; 1:10000 dilution, Sigma) and chick anti-MAP2 antibody. As secondary antibodies for anti-Tyr-T and anti-Ace-T antibodies, Alexa Fluor 488- or 594-conjugated goat anti-rat IgG (1:500 dilution, Life Technologies) and Alexa Fluor 488-conjugated goat anti-mouse IgG were used. F-actin and G-actin were labeled by rhodamine-phalloidin and fluorescent DNase I (1:500 dilution, Life Technologies), respectively. Z-stack images of stained neurons were taken at 63x with the confocal laser scanning microscope. Fluorescence intensities of Tyr-T, Ace-T and G-actin and the ratio of the fluorescence intensity of Tyr-T versus Ace-T (Tyr-T/Ace-T) were then measured in growth cone periphery by ImageJ. The numbers of growth cone in each analysis are shown in Table 1.

Time-lapse analysis

Cortical neurons were cultured in Neurobasal Medium with 2% B-27 supplement, 0.5 mM L-glutamine and 25 μ g/ml penicillin/streptomycin (the basal medium) at a density of 2×10^4 cells/cm² in glass-based 35 mm dish (Iwaki, Asahi Glass Co., Tokyo, Japan). At 4DIV, the culture dish was set in a heat stage (37°C, 5% CO₂) of the confocal laser scanning microscope. Z-stack images of cultured neurons were captured at 40x using differential interference contrast (DIC) microscopy. Fig. 5 shows the experimental paradigm. During the pre-treatment period, cortical neurons were cultured in the basal

medium for 30 minutes. Then DOI was added at the final concentration of 100 nM for 60 minutes (treatment period). In the control group, the basal medium was added instead of DOI. DIC images of identified neurons were captured every 30 seconds during the 10-minute intervals; two intervals (5-15 minute, 20-30 minute) in the pre-treatment period, and four intervals (5-15 minute, 20-30 minute, 35-45 minute, 50-60 minute) in the treatment period. To examine the morphological dynamics of dendritic growth cones, the width index (head width/neck width) was calculated every 30 seconds from captured images, and the gross changes (both increase and decrease) of all the width indexes were summed up in each 10-minute interval. The gross changes of the width index in each interval were compared with those in 5-15 minute interval of the pre-treatment period as 100%. A few growth cones (less than 10%) showed that the gross changes of the width index in 5-15 minute interval of the pre-treatment period were extremely high (more than 20). These growth cones were excluded from the analyses.

DiI-labeled dendritic growth cone *in vivo*

Rats were perfused by 4% PFA at P0 and brains were immersed at 4°C in the same fixative. The fixed brain was embedded in 1.5% agar gel in 0.1 M phosphate buffered saline and cut into 100 µm coronal slices using the vibration microtome (Linearslicer PRO7, Dosaka EM, Kyoto, Japan). Small crystals of the lipophilic tracer 1,1'-dioctadecyl-3,3,3',3'-tetramethylindocarbocyanine perchlorate (DiI; Life Technologies) were inserted into the cortical slices. The slices were incubated in 1%

PFA at 37°C for 2-4 days. Images of DiI-labeled dendritic growth cones were taken at 40x with the confocal laser scanning microscope.

Statistical analysis

All the analyses except for the time-lapse analysis were executed blind to the treatment conditions. Statistical analyses were performed by ANOVA followed by post hoc analysis (Fisher's protected least significant difference test). Differences were considered significant if the probability of error was less than 5%. All the data were expressed as the mean \pm SEM.

RESULTS

The distribution of cytoskeletons in dendrites

To examine the distribution of cytoskeletons in dendrites, cortical neurons were stained by antibodies against MAP2 and β -tubulin in combination with rhodamine-phalloidin (Fig. 6). F-actin was distributed in somatic protrusions, dendritic shaft protrusions and dendritic growth cones along with cell bodies and dendritic shafts. In contrast, MAP2 was distributed in cell bodies and dendritic shafts, but was scarce in somatic protrusions and dendritic shaft protrusions. The expression of MAP2 in dendritic growth cones was diminished gradually toward the tip. β -tubulin was widely distributed compared with MAP2, but was mostly absent in some somatic protrusions and dendritic shaft protrusions.

Expression of 5-HT1A and 5-HT2A receptors

I examined the localization of 5-HT1A and 5-HT2A receptors in cortical neurons cultured for 4 days. Neurons were immunostained by antibodies against 5-HT1A or 5-HT2A receptor in combination with rhodamine-phalloidin labeling. All neurons showed the immunoreactivity for both 5-HT1A and 5-HT2A receptors in cell bodies and dendrites (Fig. 7A, B). In dendrites, 5-HT1A receptor was expressed strongly in dendritic shafts but weakly in dendritic branches and growth cones (Fig. 7A). In contrast, the 5-HT2A receptor was expressed in dendritic shaft protrusions (dsp in Fig.

7C), dendritic growth cones (gc in Fig. 7C) and somatic protrusions (sp in Fig. 7C) in addition to dendritic shafts and branches (Fig. 7B).

Effects of 5-HT_{1A} and 5-HT_{2A/2C} receptor agonists on the dendrite formation

First, I examined the roles of 5-HT_{1A} and 5-HT_{2A/2C} receptors in the dendrite formation. Cortical neurons were cultured for 4 days and treated for 4 or 24 hours by 8-OH DPAT, DOI or 5-HT (1, 10 and 100 nM). After immunostaining with the antibody against MAP2, the dendrite formation was analyzed (Fig. 8A). 8-OH DPAT decreased significantly the number of primary dendrites by both the 4-hour treatment (11 and 13% decrease by 10 and 100 nM 8-OH DPAT, respectively) and the 24-hour treatment (15% decrease by 100 nM 8-OH DPAT) (Fig. 8B, C). The 4-hour treatment of DOI decreased the number of primary dendrites (7% decrease by 10nM DOI), the average dendrite length (13% decrease by 1 nM DOI) and the branching index (18% decrease by 100 nM DOI) (Fig. 8D), whereas the 24-hour treatment of DOI increased the number of primary dendrites significantly (9% increase by 1nM DOI) and the average dendrite length marginally (11% increase by 10 nM DOI) (Fig.8E).

5-HT showed reverse effects as compared with those of DOI. The 4-hour treatment of 5-HT increased the average dendrite length (12, 13 and 13% increase by 1, 10 and 100 nM 5-HT, respectively) and the branching index (79% increase by 10 nM 5-HT) (Fig. 8F). In contrast, the 24-hour treatment of 5-HT decreased the number of primary dendrites (10% decrease by 1 nM 5-HT) and the average dendrite length (22 and 17% decrease by 10 and 100 nM 5-HT, respectively) (Fig.8G).

Effects of 5-HT1A and 5-HT2A/2C receptor agonists on dendritic growth cone periphery and protrusions

Next, I examined the roles of 5-HT1A and 5-HT2A/5-HT2C receptors in the F-actin-rich and MAP2-negative structures in dendrites. I analyzed the length of growth cone periphery, the density of dendritic shaft protrusions and the number of somatic protrusions (Fig. 4A). 8-OH DPAT decreased the length of growth cone periphery at 10 nM by 18% (Fig. 9B). In contrast, DOI (1, 10 and 100 nM) increased the length of growth cone periphery by 27, 36 and 82%, respectively (Fig. 9A, C). Both 8-OH DOAT and DOI had no effect on the density of dendritic shaft protrusions and the number of somatic protrusions (Fig. 9B, C). Next, to determine whether the effects of DOI were mediated by 5-HT2A or 5-HT2C receptor, cortical neurons were treated for 4 hours by 100 nM DOI with or without 1000 nM 5-HT2A receptor antagonist (ketanserin). The increase of the length of growth cone periphery by DOI was reversed by the concomitant treatment of ketanserin (Fig. 9D). The treatment of ketanserin alone had no effect.

In order to investigate the morphological changes of dendritic growth cones by DOI treatment in more detail, the width index (the ratio of head width/neck width; Fig. 4B) and area of dendritic growth cone periphery were analyzed. DOI (1, 10 and 100 nM) increased the width index by 15, 10 and 20%, respectively (Fig. 9E). 100 nM DOI also increased the area by 11% (Fig. 9E). These results suggest that 5-HT2A receptor increased the size (length, width and area) of growth cone periphery.

To compare the actions of DOI, we examined those of 5-HT on the F-actin-rich and MAP2-negative structures. The 4-hour treatment of 5-HT had no effects on the length of

growth cone periphery, the density of dendritic shaft protrusions and the number of somatic protrusions (Fig. 10A), but 5-HT (1, 10 and 100 nM) increased the width index of growth cone periphery by 7, 12 and 10%, respectively (Fig. 10B). 10 nM 5-HT also increased the area of growth cone periphery by 22% (Fig. 10B).

Effects of 5-HT_{2A/2C} receptor agonist on the MT dynamics and the actin depolymerization in dendritic growth cone periphery

To examine the involvement of cytoskeletons in the effects of DOI on growth cone periphery, I focused on Tyr-T and Ace-T, which are enriched in dynamic MTs and stable MTs, respectively. Cortical neurons were cultured for 4 days and were treated with DOI for 4 hours. They were then immunostained by antibodies against Tyr-T and Ace-T, and the mean fluorescence intensity was measured. 1 nM DOI increased the intensity of Tyr-T fluorescence by 11% in growth cone periphery (Fig. 11A, D), whereas 10 nM DOI decreased the intensity of Ace-T fluorescence by 5% (Fig. 11B, D). In addition, 1 and 100 nM DOI increased the ratio of Tyr-T to Ace-T fluorescence (Tyr-T/Ace-T) in growth cones by 11 and 8%, respectively (Fig. 11C, D). The DOI-induced increase in the ratio of Tyr-T/Ace-T was reversed by the concomitant treatment of ketanserin (Fig. 11E). These results indicate that DOI increased dynamic MTs while decreased stable MTs in growth cones, suggesting that 5-HT_{2A} receptor promotes the dynamics of MTs in the dendritic growth cones.

I also compared the effects of 5-HT on the expression of Tyr-T and Ace-T in growth cone periphery with those of DOI. 100 nM 5-HT increased the intensity of Tyr-T

fluorescence by 6%, whereas 5-HT had no effect on the intensity of Ace-T fluorescence (Fig. 11F).

In the axonal growth, the motility at the leading edge of growth cones is controlled by modulating the rate of the actin polymerization (Luo, 2002). I then investigated the expression level of actin monomers (G-actin) in dendritic growth cone periphery of DOI treated neurons (Fig. 12A). 1 and 100 nM DOI increased the fluorescence intensity of G-actin by 11 and 7%, respectively (Fig. 12B). This shows that DOI increased the rate of the depolymerization of actin in dendritic growth cone periphery.

Effects of 5-HT_{2A/2C} receptor agonist on the dynamic change of the dendritic growth cone morphology

To examine whether the above effects of DOI on cytoskeletons affect the dynamics of dendritic growth cones, the morphological changes of dendritic growth cones were observed using time-lapse imaging (Fig. 13A). The gross changes of the width index (head width/neck width) of dendritic growth cones in each interval were compared. 100 nM DOI increased the gross changes of the width index at 5-15 minute and 50-60 minute intervals in the treatment period as compared with the control in the same intervals (Fig. 13B). These results suggest that DOI increased the morphological dynamics of growth cones.

The dendritic growth cone morphology *in vivo*

To examine whether the dendritic growth cone morphology observed in the present study may represent their morphology *in vivo*, cortical neurons at P0 were labeled by DiI (Fig. 14A). Pyramidal neurons showed dendritic growth cones of various morphologies; from thin to wide ones (Fig. 14B-E). These morphologies were similar to those of dissociated cortical neurons (Fig. 14F-I).

DISCUSSION

I investigated the roles of 5-HT_{1A} and 5-HT_{2A} receptors in the dendrite development of rat cortical neurons *in vitro*, with special reference to the dendrite growth cone morphology and dynamics. 5-HT_{2A/2C} receptor agonist increased the size of dendritic growth cone periphery and the morphological dynamics. In contrast, 5-HT_{1A} receptor agonist decreased the length of growth cone periphery. 5-HT itself had similar effects to those of 5-HT_{2A/2C} receptor agonist. The effects of 5-HT_{2A/2C} receptor agonist on the dendritic growth cone periphery morphology and dynamics may be mediated through the regulation of cytoskeletal proteins because the agonist increased dynamic tubulins and depolymerized actin in the dendritic growth cone periphery.

The type of cultured neurons

In the rat cerebral cortex on E16, neuronal progenitors which differentiate into neurons in the superficial layers (II-IV) still divide at the VZ while those for the deep layers (V-VI) begin to differentiate (Berry et al., 1964; Bayer et al., 1991; Ignacio et al., 1995). Because I used E16 cortex and removed proliferating cells by Ara-C at 1DIV, it is highly possible that most cells in the present study are the layer V-VI neurons (Hayashi et al., 2010).

Effects of 5-HT receptors on dendritic growth cone periphery

I categorized F-actin-positive and MAP2-negative structures into three types (dendritic growth cone periphery, dendritic shaft protrusions, and somatic protrusions), and examined roles of 5-HT_{1A} and 5-HT_{2A} receptors in these morphology and dynamics. 8-OH DPAT decreased the length of growth cone periphery. Because the expression of 5-HT_{1A} receptor was very weak in growth cones, this effect may be indirect on growth cone periphery. In contrast, DOI increased the length, width index and area of growth cone periphery. Because the increase of the length was reversed by the concomitant treatment of 5-HT_{2A} receptor antagonist, it is possible that 5-HT_{2A} receptor is involved in this increase. In addition, the present immunocytochemical study showed that 5-HT_{2A} receptor was expressed in dendritic growth cones, as well as cell bodies and dendritic shafts. The similar widespread expression of 5-HT_{2A} receptor has been reported by previous studies showing that 5-HT_{2A} receptor is expressed in cell bodies, dendritic shafts and dendritic protrusions including spines in cortical neurons (Miner et al., 2003; Jones et al., 2009; Yoshida et al., 2011). Taken together of the actions of the agonist and antagonist with the expression of 5-HT_{2A} receptor, it was suggested that 5-HT_{2A} receptor increases the size of dendritic growth cone periphery by acting directly on growth cones or indirectly through cell bodies and/or dendritic shafts.

I also examined the effects of 5-HT on dendritic growth cone periphery, dendritic shaft protrusions and somatic protrusions to investigate the specificity of those of DOI. 5-HT showed similar effects as compared with those of DOI, by increasing the width and area of growth cone periphery. These results suggest that the actions of 5-HT on the growth cone periphery may be mediated by 5-HT_{2A} receptor.

The regulation of cytoskeletal proteins by 5-HT_{2A} receptor

In MT, the polymerization and depolymerization occur rapidly in the plus end where Tyr-T is enriched, while the depolymerization occurs slowly in the minus end where Ace-T is enriched (Li and Black, 1996; Dent and Kalil 2001; Dent and Gertler, 2003; Conde and Caceres, 2009; Poulain and Sobel, 2010). In the present study, I examined effects of DOI treatment on MTs of dendritic growth cone periphery and showed that DOI increased the intensity of Tyr-T immunofluorescence and decreased the intensity of Ace-T immunofluorescence. Therefore, DOI may make MTs in dendritic growth cones more dynamic state by both the increase of dynamic MT (Tyr-T) and the decrease of stable MT (Ace-T). The positive regulation of Tyr-T expression by 5-HT was recently reported by showing that *in vivo* 5-HT depletion reduced Tyr-T in the adult rat brain (Crespi, 2010). I also showed that 5-HT increased Tyr-T in the growth cone periphery of cultured embryonic cortical neurons. Taken together, the present study showed that 5-HT may increase Tyr-T in the dendritic growth cones of cortical neurons through 5-HT_{2A} receptor.

Recently, it was reported that MTs are present in dendritic spines and dynamic MT plays important roles in the spine morphology and the synaptic plasticity (Hu et al., 2008; Conde and Caceres, 2009; Penzes et al., 2009). The research in mature hippocampal neurons using EB3 which binds to dynamic MT plus ends reported that EB3 entry into spines increases the spine size in minutes, while EB3 depletion causes the increase of filopodia and the decrease of spines in hours by affecting the actin polymerization. These results suggest the necessity of dynamic MTs for the spine morphology and the synaptic plasticity (Gu et al., 2008; Jaworski et al., 2009). In

dendritic spines of cortical neurons, the spine size is increased in 30 minutes by DOI (Jones et al., 2009). Moreover, our previous study showed that cortical neurons treated by DOI for 24 hours increased the number of spines and decreased the number of filopodia (Yoshida et al., 2011). It is likely that MT dynamics induced by DOI is also involved in the dendritic spine formation. Taken together, it was suggested that 5-HT_{2A} receptor acutely regulates both the growth cone periphery and spine morphology of cortical dendrites through the promotion of MT dynamics. In the axonal growth cone, it was reported that calcium/calmodulin (CaM)-dependent protein kinase (CaMKII) which is a mediator of the calcium-linked signaling increases MT dynamics (Schulman and Hanson, 1993; Soderling et al., 2001; Li et al., 2013). Because 5-HT_{2A} receptor is coupled to G_q protein and elicits calcium activity (Bockaert et al., 2006; Filip and Bader, 2009; Pytliak et al., 2011), it is possible that 5-HT_{2A} receptor induces MT dynamics in the dendritic growth cone through the calcium signaling pathway.

Furthermore, the present study showed the increase of G-actin by DOI in growth cone periphery, suggesting the promotion of the actin depolymerization. In F-actin bundles of axonal growth cones, there are the barbed end facing leading edge and the pointed end facing the transitional zone, and the severing and depolymerization of actin occur in the pointed end in process of F-actin treadmilling (Mitchison and Kirschner, 1988; Luo, 2002; Lowery and Vactor, 2009). The study on the family of actin depolymerizing factor ADF/cofilin reported that ADF/cofilin-mediated F-actin severing drives the actin retrograde flow and organizes the space for the protrusion and bundling of MTs, and then the neurite formation is facilitated (Flynn et al., 2012). Also, MT dynamics are important for the actin morphology in growth cones. The individual dynamic MTs which extend toward the leading edge act as the steering of the axonal

growth cone guidance and supporting F-actin bundles (Zhou and Cohan, 2004; Geraldo and Gordon-Weeks, 2009; Lowery and Vactor, 2009). My data provide the possibility that increasing the actin depolymerization by DOI may construct the space for extending toward the leading edge of dynamic MTs, and it may trigger the morphological (length and width) changes of growth cone periphery. In addition, the time-lapse analysis showed that the gross changes of the width index were higher in dendritic growth cones of neurons treated with DOI than control, suggesting that DOI may increase the dynamics of dendritic growth cones. The previous study indicated that 5-HT_{1A} receptor reduces the actin polymerization and dynamics of dendritic growth cones in hippocampal neurons (Ferreria et al., 2010). This report and the present study suggest that the effects of 5-HT_{2A/2C} receptor on dendritic growth cones are opposite to those of 5-HT_{1A} receptor. Actually, we showed previously that 5-HT_{2A} receptor has antagonistic effects on the spine formation compared with 5-HT_{1A} receptor (Yoshida et al., 2011). Although little is known about how 5-HT receptors regulate MTs and actin in the dendrite development, the present results suggest that 5-HT_{2A} receptor induces the morphological changes and increases the dynamics of dendritic growth cone through the MT dynamics and the actin depolymerization.

Effects of 5-HT and 5-HT receptors on the dendrite formation

I examined whether the effects on the growth cone periphery may lead to the dendrite formation. 8-OH DPAT decreased the number of primary dendrites, suggesting that the dendrite initiation may be inhibited via 5-HT_{1A} receptor and that the 8-OH

DPAT-induced decrease of length of growth cone periphery may not directly lead to the dendrite formation. DOI had differential effects on the dendrite formation, depending on the duration of the treatment. Thus, the short treatment (4 hours) inhibited the dendrite initiation (the number of primary dendrites), the dendrite elongation (the average dendrite length) and the dendrite arborization (the branching index). In contrast, the longer treatment (24 hours) promoted the dendrite initiation, and possibly the dendrite elongation. These results suggest that the DOI-induced growth cone dynamics may lead to the promotion of the dendrite formation in 24 hours. The differences in the effects between 4- and 24-hour treatment may be due to the non-genomic and genomic effects, respectively.

When compared with the effects of DOI, 5-HT had the reverse effects, showing the promotion of the dendrite formation by the short treatment and the inhibition by the longer treatment. These results suggest that other 5-HT receptor(s) than 5-HT_{2A} receptor has major effects on the dendrite formation by 5-HT. Our previous study showed that 5-HT₃ receptor is expressed in embryonic cortical neurons (Hayashi et al., 2010). The mRNAs of 5-HT_{1F}, 5-HT_{2B} and 5-HT_{5A} receptors are expressed in the cerebral cortex of rat embryos (Garcia-Alcocer et al., 2005, Personal communication with Dr. Shiga). It may be possible that these 5-HT receptors mediate the effects of 5-HT.

Roles of the dendritic growth cone dynamics *in vivo*

Dendritic growth cones of cultured cortical neurons show various morphologies which

are similar to those *in vivo*, but several guidance molecules for dendrites may be lost *in vitro*. Dendrites, like axons, respond to guidance cues to steer toward their targets (Scott and Luo, 2001; Jan and Jan, 2003; Kim and Chiba, 2004; Georges et al., 2008). Semaphorin 3A (Sema3A) acts as an attractant for dendrites and direct the extension of apical dendrites toward the pial surface in the cerebral cortex (Polleux et al., 2000). In addition, the dendrite length and branching of pyramidal neurons are decreased in the cortical slice of Sema3A null mice (Fenstermaker et al., 2004). Slit1 is expressed in deep cortical layers and the subplate from late embryonic days to early postnatal days and leads to the increase of the dendrite elongation and branching in cortical neurons (Whitford et al, 2002). Neurotrophins such as nerve growth factor, brain-derived neurotrophic factor, NT-3 and NT-4, and their receptors are highly expressed in the cerebral cortex during the dendrite development, and regulate the dendrite elongation and branching of cortical pyramidal neurons layer-specifically (Kimberley McAllister et al., 1995; Wirth et al., 2003; Miyashita et al., 2010; Park and Poo, 2013). It is probable that the dendritic growth cone dynamics promoted by DOI may respond to guidance cues and have influences on the dendrite elongation and arborization of cortical neurons. It remains to be examined whether these guidance molecules exist in the present dissociation culture. It is also interesting to examine interactions between 5-HT/5-HT2A receptor and these guidance molecules/their receptors in the dendrite formation of cortical neurons.

CONCLUSION

The roles of 5-HT receptors in the dendrite formation were largely unknown. In the present study, I examined the roles of 5-HT receptors in the dendritic growth cones of cerebral cortical neurons using pharmacological technique *in vitro*. I showed that 5-HT_{2A} receptor enlarged the dendritic growth cone periphery. Moreover, the time-lapse analysis revealed that 5-HT_{2A} receptor induced the dynamics of dendritic growth cone morphology. Concomitantly, 5-HT_{2A} receptor promoted MT dynamics and actin depolymerization in growth cone periphery. These changes in the dynamics and polymerization of cytoskeletons may underlie the molecular bases for the morphological changes of the dendrite growth cones. Although the physiological significance of 5-HT_{2A} receptor in the dendritic growth cones remains to be examined, the present study provides important data to understand the roles of 5-HT receptors in the dendrite development. In addition, considering that there are limited studies on the regulation of dendrite formation by extracellular factors such as neurotrophins and guidance molecules, the present study may give a clue to elucidate the molecular mechanism of the dendrite formation in the brain.

ACKNOWLEDGMENTS

I wish to thank Prof. Takashi Shiga, Associate Prof. Tomoyuki Masuda and Assistant Prof. Kouji Senzaki at University of Tsukuba for instructions and advices, and members of the laboratory for various supports in this research.

REFERENCES

Aitken A.R., Tork I. (1988) Early development of serotonin-containing neurons and pathways as seen in wholemount preparations of the fetal rat brain. *J. Comp. Neurol.* 274:32-47.

Altman J., Bayer S.A. (1990) Vertical compartmentation and cellular transformations in the germinal matrices of the embryonic rat cerebral cortex. *Exp. Neurol.* 107:23-35.

Amargos-Bosch M., Bortolozzi A., Victoria Puig M., Serrats J., Adell A., Celada P., Miklos T., Mengod G., Artigas F. (2004) Co-expression and in vivo interaction of serotonin 1A and serotonin 2A receptors in pyramidal neurons of prefrontal cortex. *Cereb. Cortex* 14:281-299.

Barnes N.M., Sharp T. (1999) A review of central 5-HT receptors and their function. *Neuropharmacology* 38:1083-1152.

Bass P.W., Black M.M., Banker G.A. (1989) Change in microtubule polarity orientation during the development of hippocampal neurons in culture. *J. Cell Biol.* 109:3085-3094.

Bayer S.A., Altman J. (1990) Developmental of layer and the subplate in the rat neocortex. *Exp. Neurol.* 107:48-62.

Bayer S.A., Altman J., Russo J.R., Dai X., Simmons A.J. (1991) Cell migration in the

rat embryonic neocortex. *J. Comp. Neurol.* 307:499-516.

Berry M., Rogers A.W., Eayrs J.T. (1964) Pattern of cell migration during cortical histogenesis. *Nature* 203:591-593.

Bockaert J., Claeysen S., Becamel C., Dumuis A., Marin P. (2006) Neuronal 5-HT metabotropic receptor: fine-tuning of their structure, signaling, and roles in synaptic modulation. *Cell Tissue Res.* 326:553-572.

Celada P., Victoria Puig M., Artigas F. (2013) Serotonin modulation of cortical neurons and networks. *Integr. Neurosci.* 7:1-20.

Chubakov A.R., Gromova E.A., Konovalov G.V., Sarkisova E.F., Chumasov E.I. (1986) The effects of serotonin on the morpho-functional development of rat cerebral neocortex in tissue culture. *Brain Res.* 369:285-297.

Conde C., Caceres A. (2009) Microtubule assembly, organization and dynamics in axon and dendrites. *Nature Rev. Neurosci.* 10:319-332.

Crespi F. (2010) Further electrochemical and behavioural evidence of a direct relationship between central 5-HT and cytoskeleton in the control of mood. *Open Neurol. J.* 4:5-14.

Daubert E.A., Condrón B.G. (2010) Serotonin: a regulator of neuronal morphology and

circuitry. *Trends Neurosci.* 33:424-434.

Dehmelt L., Halpain S. (2004) Actin and microtubules in neurite initiation; Are MAPs the missing Link? *J. Neurobiol.* 58:18-33.

De Lima A.D., Merten M.D.P., Voigt T. (1997) Neuritic differentiation and synaptogenesis in serum-free neuronal cultures of rat cerebral cortex. *J. Comp. Neurol.* 382:230-246.

Dent E.W., Gertler F.B. (2003) Cytoskeletal dynamics and transport in growth cone motility and axon guidance. *Neuron* 40:209-227.

Dent E.W., Kalil K. (2001) Axon branching requires interactions between dynamic microtubules and actin filaments. *J. Neurosci.* 21:9757-9769.

Dooley A.E., Pappas I.S., Parnavelas J.G. (1997) Serotonin promotes the survival of cortical glutamatergic neurons in vitro. *Exp. Neurol.* 148:205-214.

Fenstermaker V., Chen Y., Ghosh A., Yuste R. (2004) Regulation of dendritic length and branching by semaphorin 3A. *J. Neurobiol.* 58:403-412.

Ferreira T.A., Iacono L.L., Gross C.T. (2010) Serotonin receptor 1A modulates actin dynamics and restricts dendritic growth in hippocampal neurons. *Eur. J. Neurosci.* 32:18-26.

Filip M., Bader M. (2009) Overview on 5-HT receptors and their role in physiology and pathology of the central nervous system. *Pharmacol. Rep.* 61:761-777.

Flynn K.C., Hellal F., Neukirchen D., Jacob S., Tahirovic S., Duprez S., Stern S., Garvalov B.K., Gurniak C., Shaw A.E., Meyn L., Wedlich-Soldner R., Bamburg J.R., Small J.V., Witke W., Bradke F. (2012) ADF/Cofilin-mediated actin retrograde flow directs neurite formation in the developing brain. *Neuron* 76:1091-1107.

Gandou C., Ohtani A., Senzaki K., Shiga T. (2010) Neurotensin promotes the dendrite elongation and the dendritic spine maturation of the cerebral cortex *in vitro*. *Neurosci. Res.* 66:246-255.

Garcia-Alcocer G., Sarabia-Altamirano G., Martinez-Torres A., Miledi R. (2004) Developmental expression of 5-HT_{5A} receptor mRNA in the rat brain. *Neurosci. Lett.* 379:101-105.

Gaspar P., Cases O., Maroteaux L. (2003) The developmental role of serotonin: news from mouse molecular genetics. *Nature Rev. Neurosci.* 4:1002-1012.

Georges P.C., Hadzimichalis N.M., Sweet E.S., Firestein B.L. (2008) The yin-yang of dendrite morphology: Unity of actin and microtubules. *Mol. Neurobiol.* 38:270-284.

Geraldo S., Gordon-Weeks P.R. (2009) Cytoskeletal dynamics in growth-cone steering.

J Cell Sci. 122:3595-3604.

Gu J., Firestein B.L., Zheng J.Q. (2008) Microtubules in dendritic spine development. *J. Neurosci.* 28:12120-12124.

Hamada S., Senzaki K., Hamaguchi-Hamada K., Tabuchi K., Yamamoto H., Yamamoto T., Yoshikawa S., Okano H., Okado N. (1998) Localization of 5-HT_{2A} receptor in rat cerebral cortex and olfactory system revealed by immunohistochemistry using two antibodies raised in rabbit and chicken. *Mol. Brain Res.* 54:199-211.

Harigai Y., Natsume M., Li F., Ohtani A., Senzaki K., Shiga T. (2011) Differential roles of calcitonin family peptides in the dendrite formation and spinogenesis of the cerebral cortex *in vitro*. *Neuropeptides* 45:263-272.

Hayashi T., Ohtani A., Onuki F., Natsume M., Li F., Satou T., Yoshikawa M., Senzaki K., Shiga T. (2010) Roles of serotonin 5-HT₃ receptor in the formation of dendrites and axons in the rat cerebral cortex: An *in vitro* study. *Neurosci. Res.* 66:22-29.

Hellendall R.P., Schambra U.B., Liu J.P., Lauder J.M. (1993) Prenatal expression of 5-HT_{1C} and 5-HT₂ receptors in the rat central nervous system. *Exp. Neurol.* 120:186-201.

Hering H., Sheng M. (2001) Dendritic spines: structure, dynamics and regulation. *Nat. Rev. Neurosci.* 2:880-888.

Hillion J., Catelon J., Riad M., Hamon M., De Vitry F. (1994) Neuronal localization of 5-HT1A receptor mRNA and protein in rat embryonic brain stem cultures. *Dev. Brain Res.* 79:195-202.

Hillion J., Milne-Edwards D.B.J., CATERON J., De Vitry J., Gros F., Hamon M. (1993) Prenatal developmental expression of rat brain 5-HT1A receptor gene followed by PCR. *Biochem. Biophys. Res. Commun.* 191:991-997.

Howard J., Hyman A.A. (2003) Dynamics and mechanics of the microtubule plus end. *Nature* 422:753-758.

Hu X., Viesselmann C., Nam S., Merriam E., Dent E.W. (2008) Activity-dependent dynamic microtubule invasion of dendritic spines. *J. Neurosci.* 28:13094-13105.

Ignacio M.P.D., Kimm E.J., Kageyama G.H., Yu J., Robertson R.T. (1995) Postnatal migration of neurons and formation of laminae in rat cerebral cortex. *Anat. Embryol.* 191:89-100.

Jan Y.-N., Jan L.Y. (2003) The control of dendrite development. *Neuron* 40:229-242.

Jaworski J., Kapitein L.C., Gouveia S.M., Dortland B.R., Wulf P.S., Grigoriev I., Camera P., Spangler S.A., Stefano P.D., Demmers J., Krugers H., Defilippi P., Akhmanova A., Hoogenraad C.C. (2009) Dynamic microtubules regulate dendritic

spine morphology and synaptic plasticity. *Neuron* 61:85-100.

Jones K.A., Srivastava D.P., Allen J.A., Strachan R.T., Roth L.B., Penzes P. (2009) Rapid modulation of spine morphology by the 5-HT_{2A} serotonin receptor through kalirin-7 signaling. *Proc. Natl. Acad. Sci. USA.* 106:19575-19580.

Kim S., Chiba A. (2004) Dendritic guidance. *Trends Neurosci.* 27:194-202.

Kimberley McAllister A., Lo D.C., Katz L.C. (1995) Neurotrophins regulate dendritic growth in developing visual cortex. *Neuron* 15:791-803.

Kriegstein A., Noctor S., Martinez-Cerdeno V. (2006) Patterns of neural stem and progenitor cell division may underlie evolutionary cortical expansion. *Nat. Rev. Neurosci.* 7:883-890.

Lanfumeey L., Hamon M. (2004) 5-HT₁ receptors. *Curr. Drug Targets CNS Neurol Disord.* 3:1-10.

Lauder J.M. (1990) Ontogeny of the serotonergic system in the rat: serotonin as a developmental signal. *Ann. NY. Acad. Sci.* 600:297-313.

Lavdas A.A., Blue M.E., Lincoln J., Parnavelas J.G. (1997) Serotonin promotes the differentiation of glutamate neurons in organotypic slice cultures of the developing cerebral cortex. *J. Neurosci.* 17:7872-7880.

Li F., Ohtani A., Senzaki K., Shiga T. (2012) Receptor-dependent regulation of dendrite formation of noradrenalin and dopamine in non-GABAergic cerebral cortical neurons. *Develop. Neurobiol.* 73:370-383.

Li L., Fothergill T., Hatchins I.B., Dent E.W., Kalil K. (2013) Wnt5a evokes cortical axon outgrowth and repulsive guidance by tau mediated reorganization of dynamic microtubules. *Develop. Neurobiol.* In press.

Li Y., Black M.M. (1996) Microtubule assembly and turnover in growing axons. *J. Neurosci.* 16:531-544.

Lidov H.G.W., Molliver M.E. (1982a) An immunohistochemical study of serotonin neuron development in the rat: ascending pathways and terminal fields. *Brain Res. Bull.* 8:389-430.

Lidov H.G.W., Molliver M.E. (1982b) Immunohistochemical study of the development of serotonergic neurons in the rat CNS. *Brain Res. Bull.* 9:559-604.

Li Q.-H., Nakadate K., Tanaka-Nakadate S., Nakatsuka D., Cui Y., Watanabe Y. (2004) Unique expression patterns of 5-HT_{2A} and 5-HT_{2C} receptors in the rat brain during postnatal development: Western blot and immunohistochemical analyses. *J. Comp. Neurol.* 469:128-140.

Lowery L.A., Vactor D.V. (2009) The trip of the trip: understanding the growth cone machinery. *Nature Rev. Mol. Cell Biol.* 10:332-343.

Lund R.D., Mustari M.J. (1977) Development of Geniculocortical pathway in rats. *J. Comp. Neurol.* 173:289-306.

Luo L. (2002) Actin cytoskeleton regulation in neuronal morphogenesis and structural plasticity. *Ann. Rev. Cell Dev. Biol.* 18:601-635.

Matus A. (2005) Growth of dendritic spines: a continuing story. *Current Opinion Neurobiol.* 15:67-72.

Matsukawa M., Nakadate K., Ishihara I., Okado N. (2003) Synaptic loss following depletion of noradrenalin and/or serotonin in the rat visual cortex: a quantitative electron microscopic study. *Neuroscience* 122:627-635.

Miner L.A.H., Backstrom J.R., Sander-Bush E., Sesack S.R. (2003) Ultrastructural localization of serotonin 2A receptors in the middle layers of the rat prelimbic prefrontal cortex. *Neuroscience* 116:107-117.

Mitchison T., Kirschner M. (1988) Cytoskeletal dynamics and nerve growth. *Neuron* 1:761-772.

Miyashita T., Wintzer M., Kurotani T., Konishi T., Ichinohe N., Rockland K.S. (2010)

Neurotrophin-3 is involved in the formation of apical dendritic bundles in cortical layer 2 of the rat. *Cereb. Cortex* 20:229-240.

Molyneaux B.J., Arlotta P., Menezes J.R.L., Macklis J. (2007) Neuronal subtype specification in the cerebral cortex. *Nat. Rev. Neurosci.* 8:427-437.

Nadarajah B., Parnavelas J.G. (2002) Modes of neuronal migration in the developing cerebral cortex. *Nat. Rev. Neurosci.* 3:423-432.

O'Leary D.D.M., Koester S.E. (1993) Development of projection neuron type, axon pathways, and patterned connections of the mammalian cortex. *Neuron* 10:991-1006.

Oostland M., Van Hooft J.A. (2013) The role of serotonin in cerebellar development. *Neuroscience* 248:201-212.

Park H., Poo M. (2013) Neurotrophin regulation of neural circuit development and function. *Nature Rev. Neurosci.* 14:7-23.

Parnavelas J.G. (2000) The origin and migration of cortical neurons: new vistas. *Trends Neurosci.* 23:126-131.

Penzes P., Srivastava D.P., Woolfrey K.M. (2009) Not just actin? A role for dynamic microtubules in dendritic spines. *Neuron* 61: 3-5.

Polleux F., Morrow T., Ghosh A. (2000) Semaphorin 3A is a chemoattractant for cortical apical dendrites. *Nature* 404:567-573.

Poulain F.E., Sobel A. (2010) The microtubule network and neuronal morphogenesis: Dynamic and coordinated orchestration through multiple players. *Mol. Cell Neurosci.* 43:15-32.

Pytliak M., Vargova V., Mechirova V., Felsoci M. (2011) Serotonin receptors – From molecular biology to clinical applications. *Physiol. Res.* 60:15-25.

Rubenstein J.L.R. (1998) Development of serotonergic neurons and their projections. *Biol. Psychiatry* 44:145-150.

Sanchez C., Diaz-Nido J., Avila J. (2000) Phosphorylation of microtubule-associated protein 2 (MAP2) and its relevance for the regulation of the neuronal cytoskeleton function. *Progress Neurobiol.* 61:133-168.

Schulman H., Hanson P.I. (1993) Multifunctional Ca²⁺/calmodulin-dependent protein kinase. *Neurochem. Res.* 18:65-77.

Scott E.K., Luo L. (2001) How do dendrites take their shape? *Nature Neurosci.* 4:359-365.

Sekino Y., Kojima N., Shirao T. (2007) Role of actin cytoskeleton in dendritic spine

morphogenesis. *Neurochem. International* 51:92-104.

Sikich L., Hickok J.M., Todd R.D. (1990) 5-HT_{1A} receptors control neurite branching during development. *Dev. Brain Res.* 56:269-274.

Soderling T.R., Chang B., Brickey D. (2001) Cellular signaling through multifunctional Ca²⁺/calmodulin-dependent protein kinase II. *J. Biol. Chem.* 276:3719-3722.

Speranza L., Chambery A., Di Domenico M., Crispino M., Severino V., Volpicelli F., Leopoldo M., Bellenchi G.C., di Porzio U., Perrone-Capano C. (2013) The serotonin receptor 7 promotes neurite outgrowth via ERK and Cdk5 signaling pathways. *Neuropharmacology* 67:155-167.

Victoria Puig M., Gullledge A.T. (2011) Serotonin and prefrontal cortex function: neurons, networks, and circuits. *Mol. Neurobiol.* 44:449-464.

Vitalis T., Cases O., Passemard S., Callebert J., Parnavelas J.G. (2007) Embryonic depletion of serotonin affects cortical development. *Eur. J. Neurosci.* 26:331-344.

Vitalis T., Parnavelas J.G. (2003) The role of serotonin in early cortical development. *Dev. Neurosci.* 25:245-256.

Whitford K.L., Marillat V., Stein E., Goodman C.S., Tessier-Lavigne M., Chedotal A., Ghosh A. (2002) Regulation of cortical dendrite development by Slit-Robo interactions.

Neuron 33:47-61.

Wirth M.J., Brun A., Grabert J., Petz S., Wahle P. (2003) Accelerated dendritic development of rat cortical pyramidal cells and interneurons after biolistic transfection with BDNF and NT4/5. *Development* 130:5827-5838.

Yoshida H., Kanamaru C., Ohtani A., Li F., Senzaki K., Shiga T. (2011) Subtype specific roles of serotonin receptors in the spine formation of cortical neurons in vitro. *Neurosci. Res.* 71:311-314.

Zhou F.-Q., Cohan C.S. (2004) How actin filaments and microtubules steer growth cones to their targets. *J. Neurobiol.* 58:84-91.

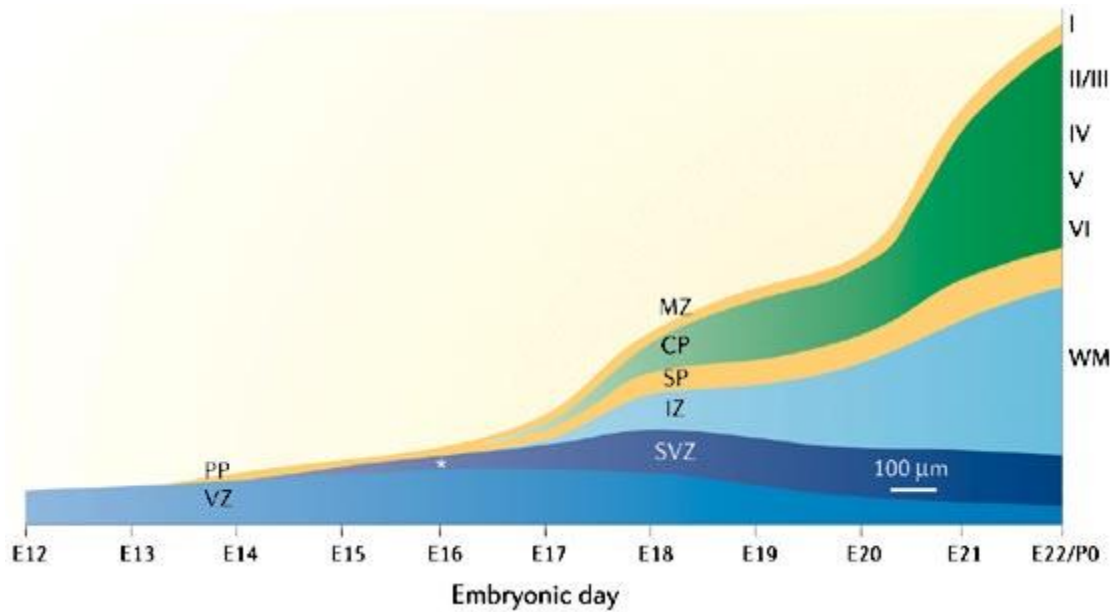


Figure 1. Histogenesis of the cerebral cortex.

The neurogenesis of the rat cerebral cortex starts from E12 and completes by E21-22. The cerebral cortex is six-layered structure, and neurons in layers VI, V, IV and II-III differentiate on E15-16, E16-17, E17-18 and E18-19, respectively. CP, cortical plate; IZ, intermediate zone; MZ, marginal zone; PP, preplate; SP, subplate; SVZ, subventricular zone; VZ, ventricular zone; WM, white matter. (adapted from Kriegstein et al., 2006, *Nature Rev. Neurosci.* 7:883-890.)

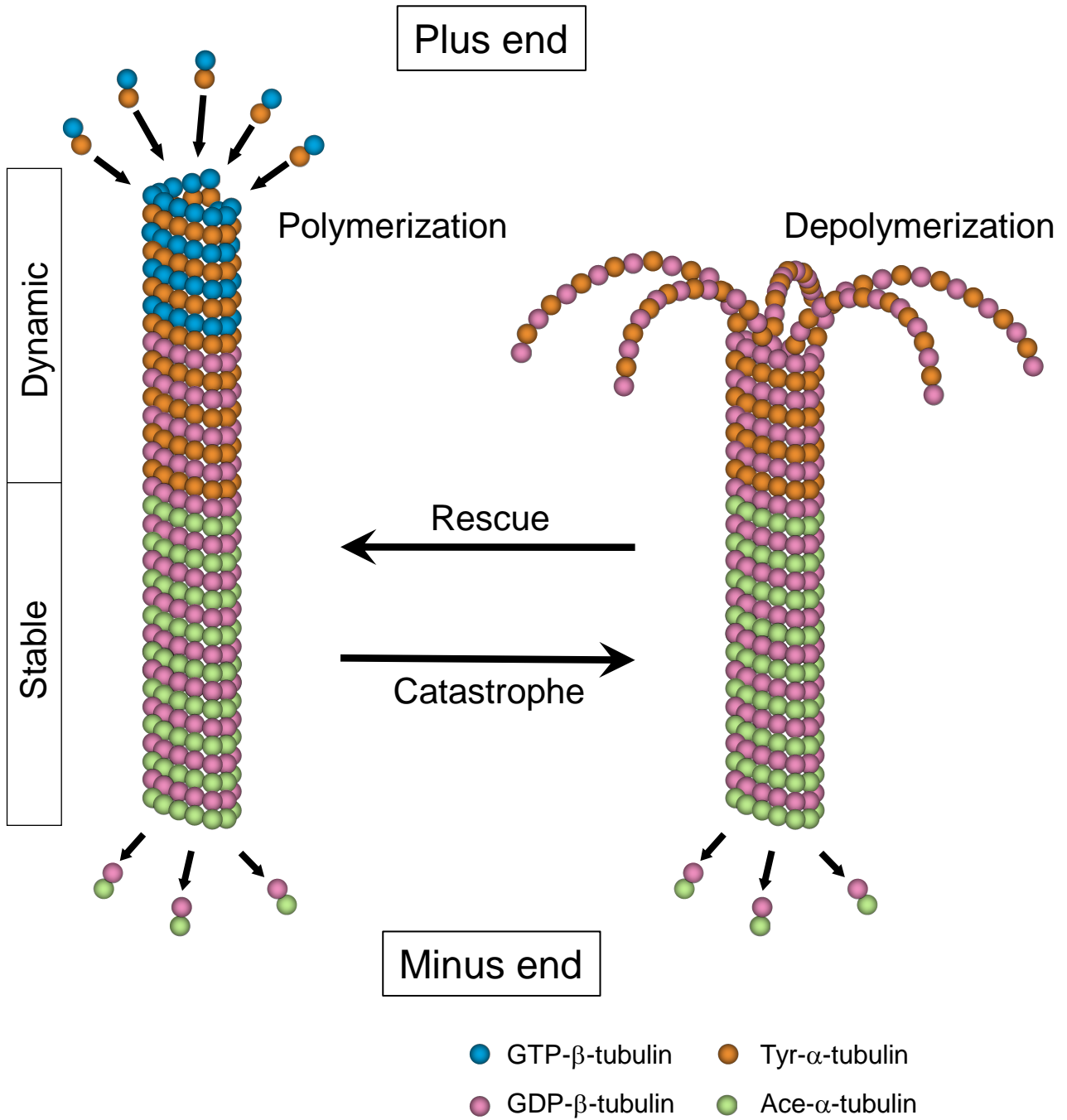


Figure 2. Architecture of microtubules.

Microtubules (MTs) are polarized structures composed of α - and β -tubulin heterodimer subunits. The highly tyrosinated (Tyr)- α -tubulin is rich in the plus end and highly acetylated (Ace)- α -tubulin in the minus end. The polymerization and depolymerization of MTs occur rapidly in the plus end, while the depolymerization occurs slowly in the minus end.

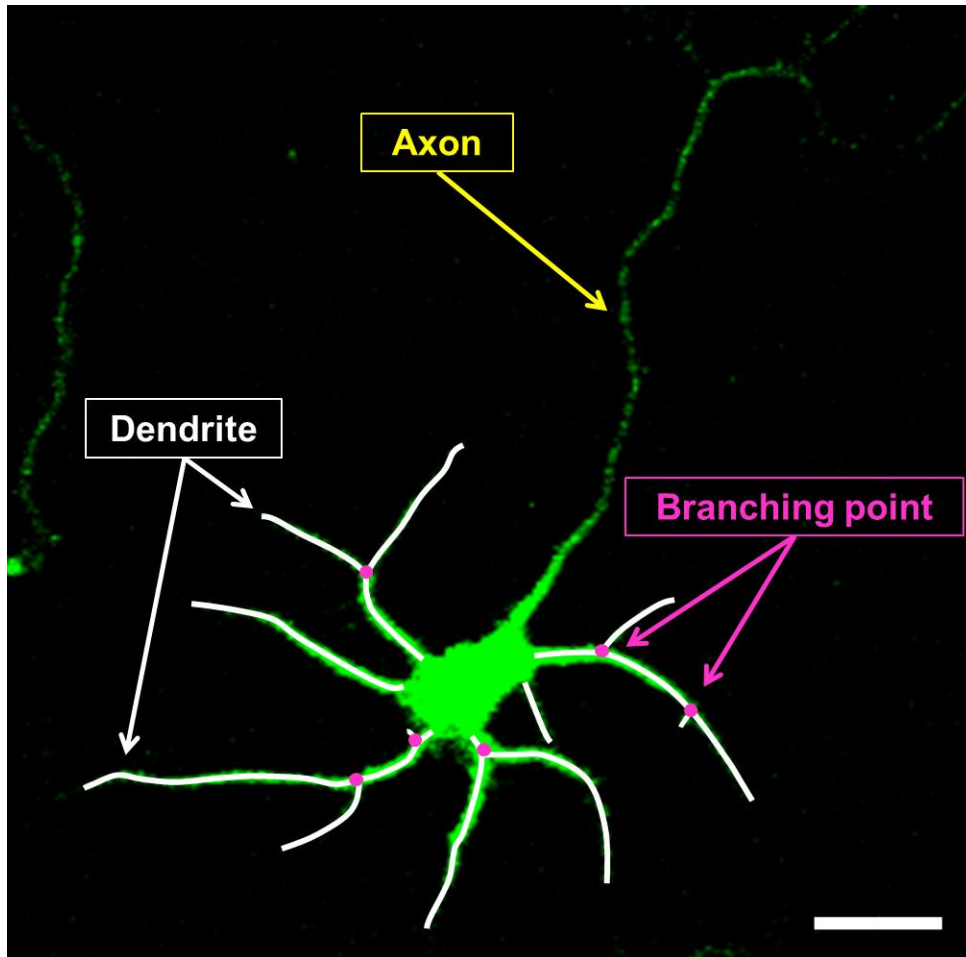


Figure 3. Analysis of the dendrite formation.

Cortical neurons were cultured for 4 days and immunostained by the antibody against MAP2. The MAP2-positive longest neurite (yellow arrow) and other shorter neurites (white lines) were identified as an axon and dendrites, respectively (Hayashi et al., 2010). Four parameters of the dendrite formation were measured; the total dendrite length (the total length of white lines), the number of the primary dendrites (number of the dendrites emerging from the cell body), the average dendrite length (total dendrite length/number of the primary dendrites) and the branching index (total number of branching points (red dots)/number of the primary dendrites). Scale bar: 20 μm .

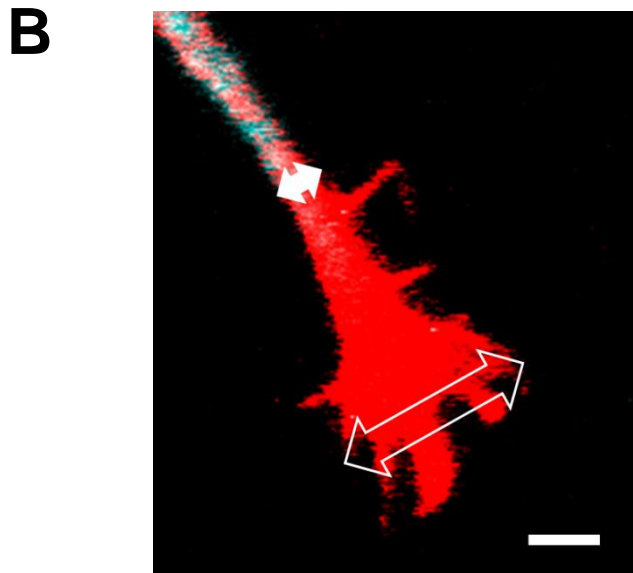
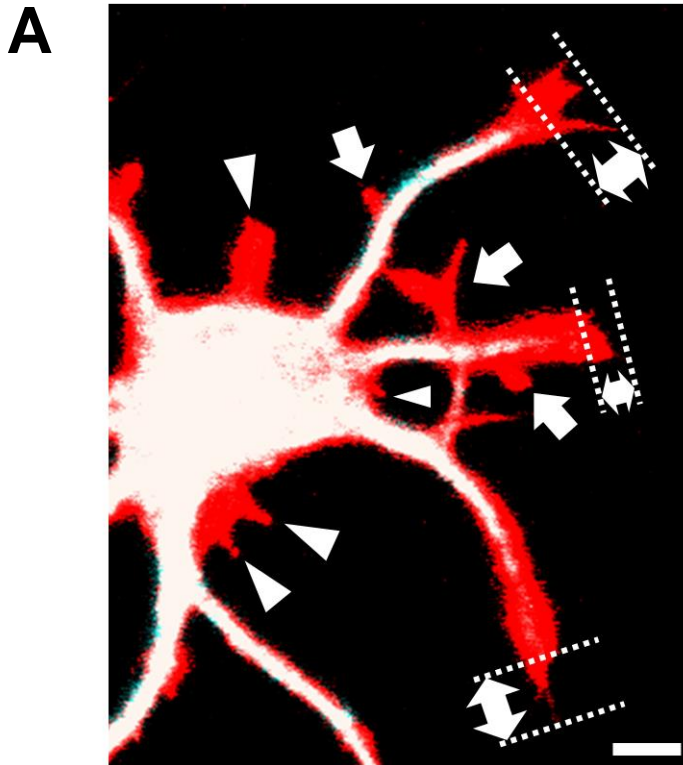


Figure 4. Analysis of dendritic growth cone periphery and protrusions. Neurons were double-stained by the anti-MAP2 antibody (blue) and rhodamine-phalloidin (red). (A) F-actin-positive and MAP2-negative structures were divided into three types, and the length of growth cone periphery (double-headed arrows), the number of dendritic shaft protrusions (arrows; thin protrusions emerging from the dendritic shaft) per unit dendrite length and the number of somatic protrusions (arrowheads; thin protrusions emerging from the cell body) per neuron were measured. (B) The width index of dendritic growth cone periphery which is the ratio of head width (open arrow) and neck width (white arrow) was measured. Scale bars: 5 μm (A), 2 μm (B)

Table 1. Numbers of growth cones, dendrites and neurons measured in each analyses. Corresponding Fig. numbers are shown.

Drug	Analyses	Target	Concentration (nM)				Fig.
			0	1	10	100	
8-OH DPAT	Dendrite formation (4 h)	Neuron	93	67	94	90	8B
	Dendrite formation (24 h)		72	53	62	70	8C
	Length of growth cone periphery	Growth cone	221	218	235	250	
	Density of dendritic shaft protrusions	Dendrite	125	122	137	150	9B
	No. of somatic protrusions	Neuron	32	34	33	33	
DOI	Dendrite formation (4 h)	Neuron	165	113	95	106	8D
	Dendrite formation (24 h)		76	72	61	95	8E
	Length of growth cone periphery	Growth cone	269	238	231	225	
	Density of dendritic shaft protrusions	Dendrite	185	180	161	149	9C
	No. of somatic protrusions	Neuron	40	37	40	37	
	Width index of growth cone periphery		336	350	359	321	9E
	Area of growth cone periphery		514	536	522	496	
	Tyr-T	Growth cone	172	168	188	156	
	Ace-T		164	181	169	167	11D
	Tyr-T/Ace-T		186	184	204	131	
G-actin		175	194	172	175	12B	
5-HT	Dendrite formation (4 h)	Neuron	83	54	66	51	8F
	Dendrite formation (24 h)		56	28	51	39	8G
	Length of growth cone periphery	Growth cone	418	337	340	359	
	Density of dendritic shaft protrusions	Dendrite	146	114	108	113	10A
	No. of somatic protrusions	Neuron	41	27	29	29	
	Width index of growth cone periphery		397	316	333	371	10B
	Area of growth cone periphery		145	121	113	132	
	Tyr-T	Growth cone	68	61	53	60	11E
	Ace-T		75	68	63	72	

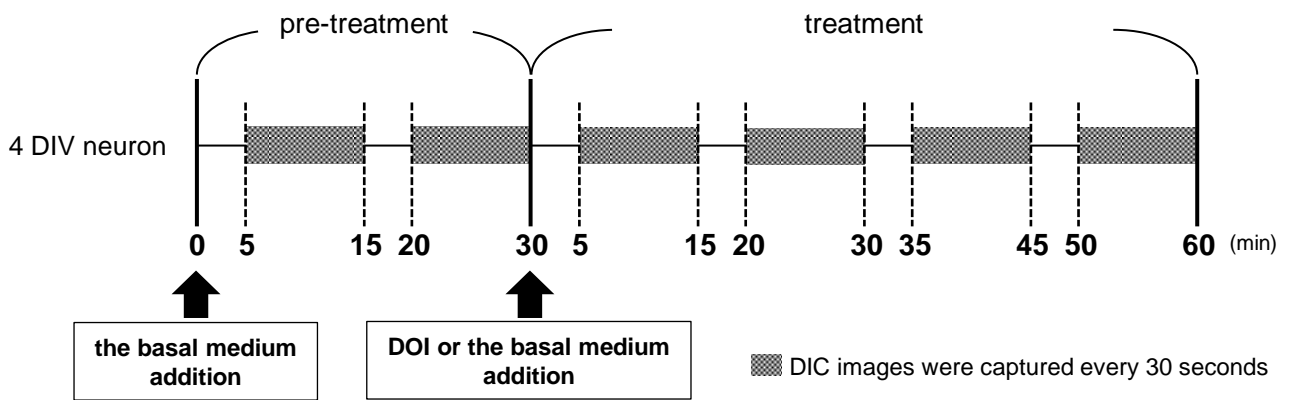


Figure 5. The experimental paradigm for the time-lapse analysis.

Cortical neurons were cultured for 4 days and the basal medium was added in the pre-treatment period. After 30 minutes, the medium was replaced with 100 nM DOI (the experimental group) or the basal medium (the control group) in the treatment period. DIC images were captured every 30 seconds during the 10 minutes-intervals (shaded periods).

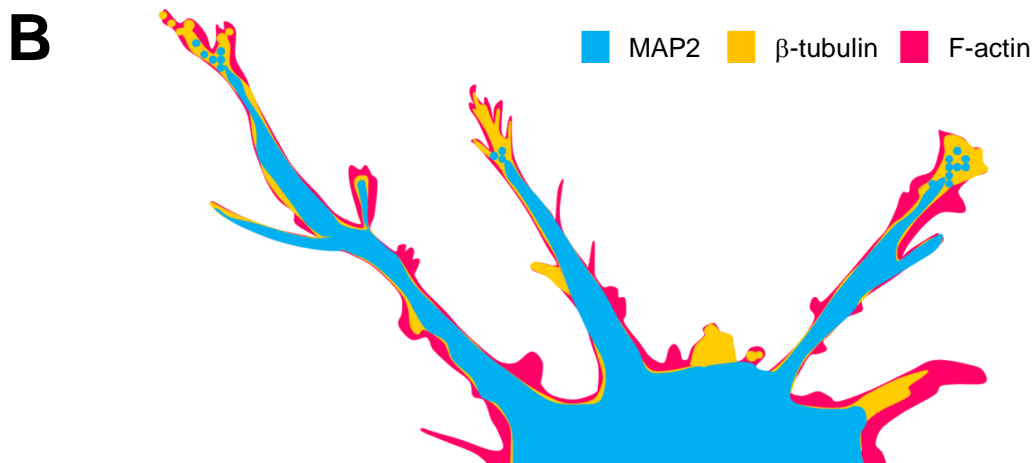
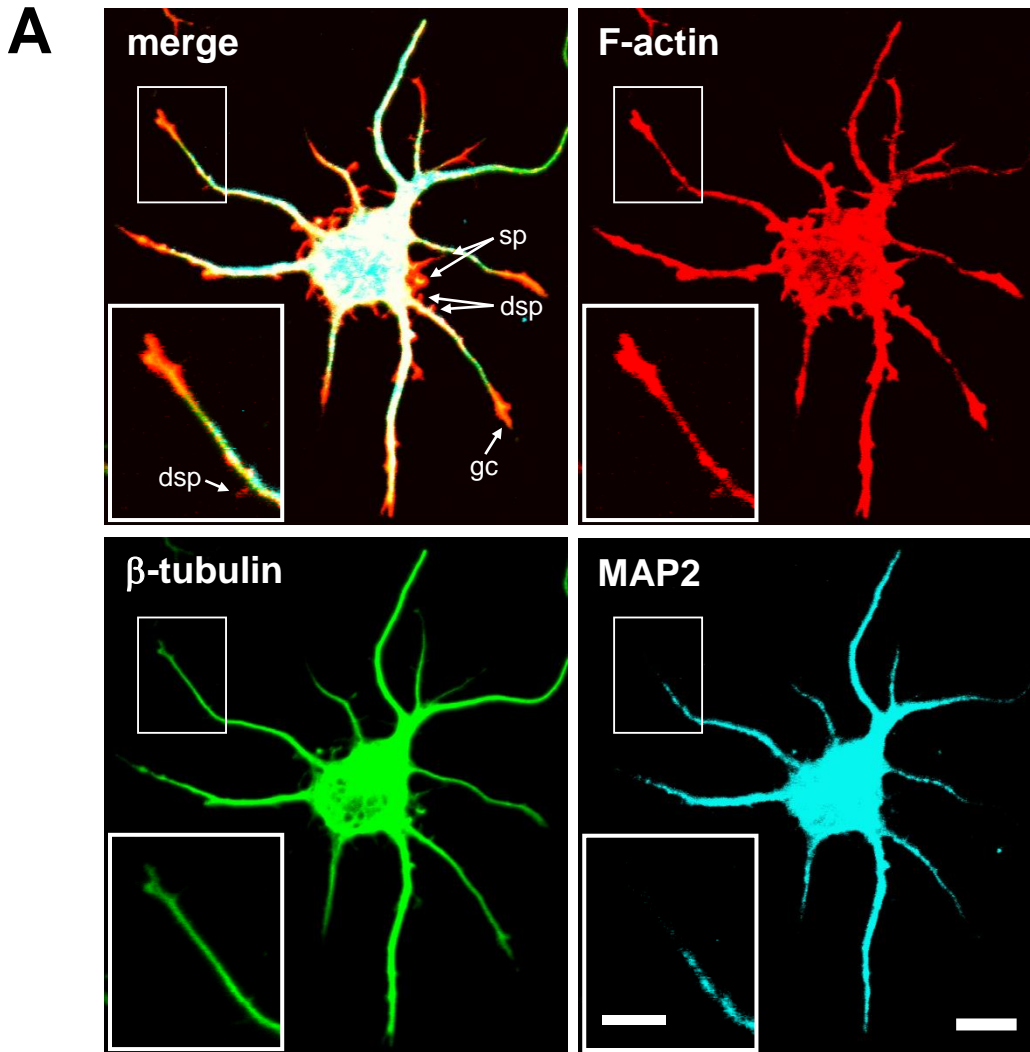


Figure 6. Cytoskeletal proteins in dendrites.

The distribution of cytoskeletal proteins in dendrites was examined. (A) Neurons cultured for 4 days were stained by the antibodies against MAP2 (blue) and β -tubulin (green) in combination with rhodamine-phalloidin which binds F-actin (red). Boxed areas in each low power view are enlarged in the insets. (B) A schematic illustration showing the distribution of the cytoskeletal proteins. F-actin (red) was distributed in the cell body, dendrites and all the protrusions. MAP2 (blue) was restricted in cell bodies and dendritic shafts, while β -tubulin (yellow) was distributed in the cores of the protrusions as well as cell bodies and dendritic shafts. dsp; dendritic shaft protrusions, gc; growth cone, sp; somatic protrusions. Scale bar: 10 μ m (A), 5 μ m (insert in A)

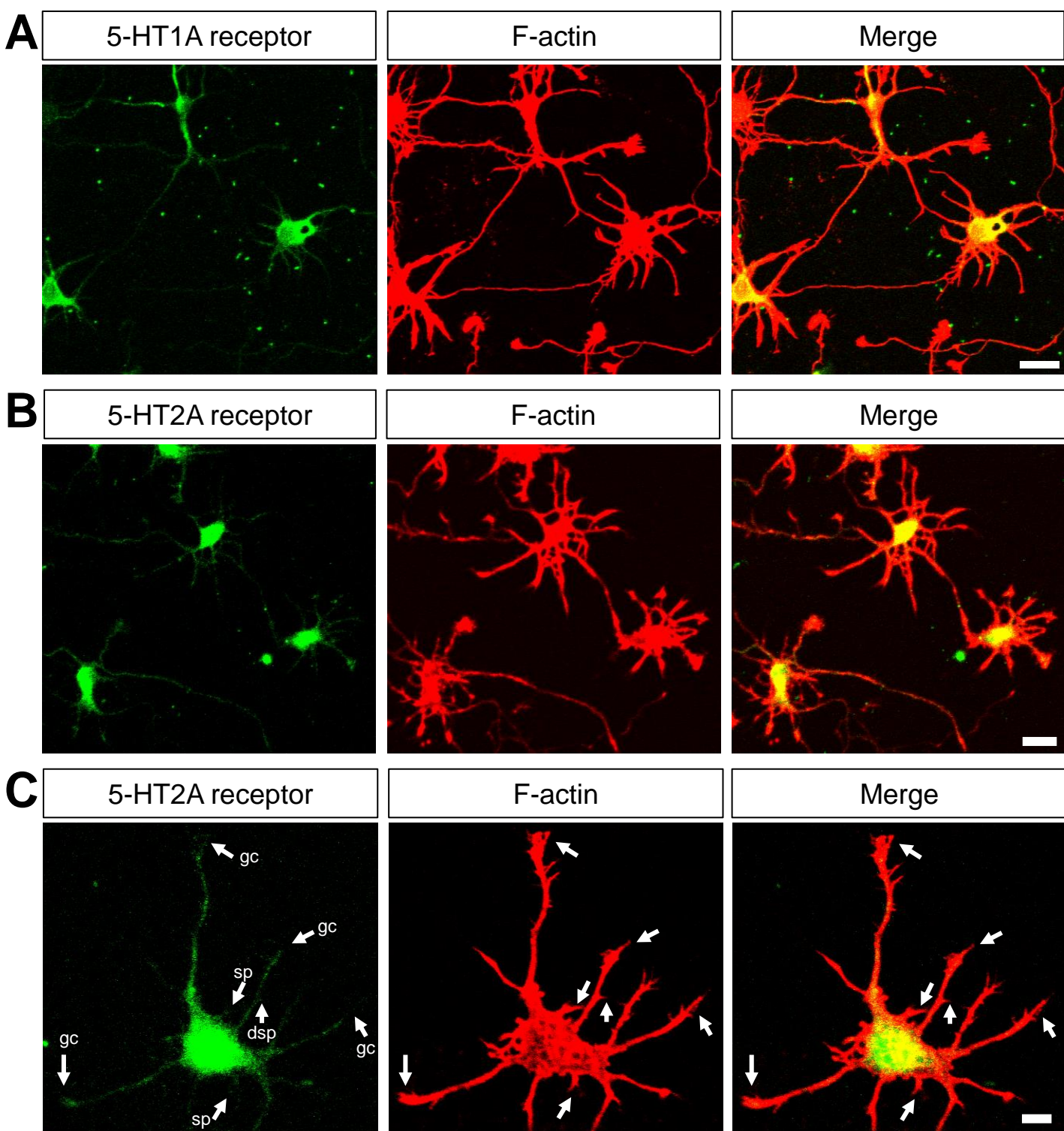


Figure 7. The expression of 5-HT1A and 5-HT2A receptors.

Cortical neurons were cultured for 4 days and double-stained by the antibodies against 5-HT1A or 5-HT2A receptor (green) and rhodamine-phalloidin (red) to localize 5-HT1A or 5-HT2A receptor and F-actin, respectively. (A) 5-HT1A receptor was expressed strongly in cell bodies and dendritic shafts of all neurons. (B) 5-HT2A receptor was expressed in cell bodies, dendritic shafts and branches of all neurons. (C) 5-HT2A receptor was present in somatic protrusions (sp), dendritic shaft protrusions (dsp) and growth cones (gc). Scale bar: 20 μ m (A, B), 5 μ m (C).

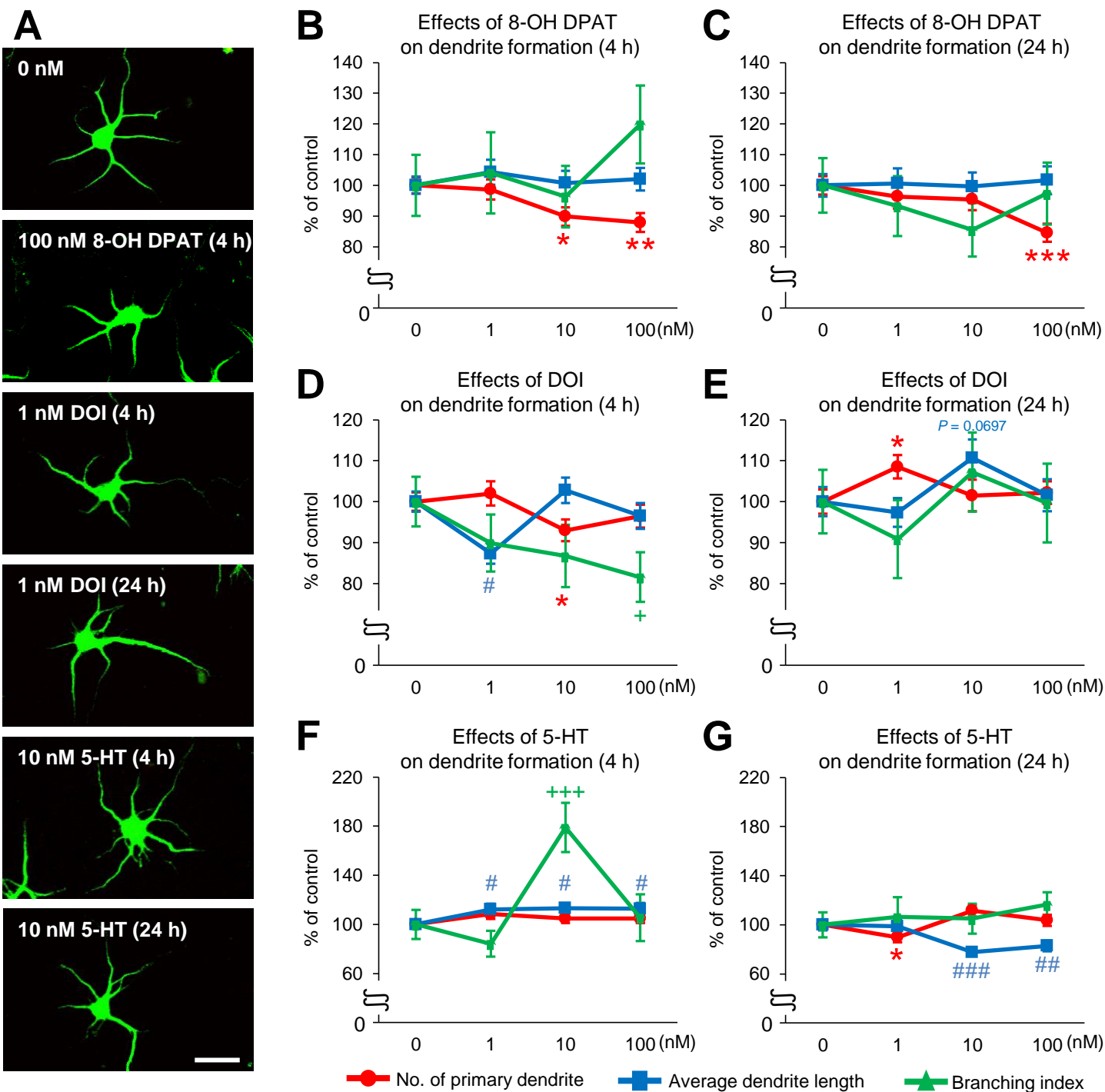


Figure 8. Effects of 8-OH DPAT, DOI and 5-HT on the dendrite formation.

Cortical neurons were cultured for 4 days and treated with 8-OH DPAT, DOI or 5-HT for 4 or 24 hours. The neurons were immunostained by anti-MAP2 and anti-GAD65/67 antibodies, and effects of agonists and 5-HT on the dendrite formation were analyzed in GAD65/67-negative neurons. (A) Typical examples of neurons treated with 8-OH DPAT, DOI or 5-HT were shown. (B, C) The quantitative analysis showed that 8-OH DPAT decreased the number of primary dendrites by both the 4 and 24 hour-treatment. (D, E) The quantitative analysis showed that the 4 hour-treatment of DOI decreased the number of primary dendrites, the average dendrite length and branching index, whereas the 24 hour-treatment of DOI increased the number of primary dendrites and the average dendrite length marginally. (F, G) The 4 hour-treatment of 5-HT increased the average dendrite length and the branching index but had no effect on the number of primary dendrites. In contrast, the 24 hour-treatment of 5-HT decreased the number of primary dendrites, the average dendrite length. Scale bar: 40 μ m. Data are shown as mean \pm SEM. * $P < 0.05$, ** $P < 0.01$, *** $P < 0.001$, # $P < 0.05$, ### $P < 0.01$, #### $P < 0.001$, + $P < 0.05$, +++ $P < 0.001$

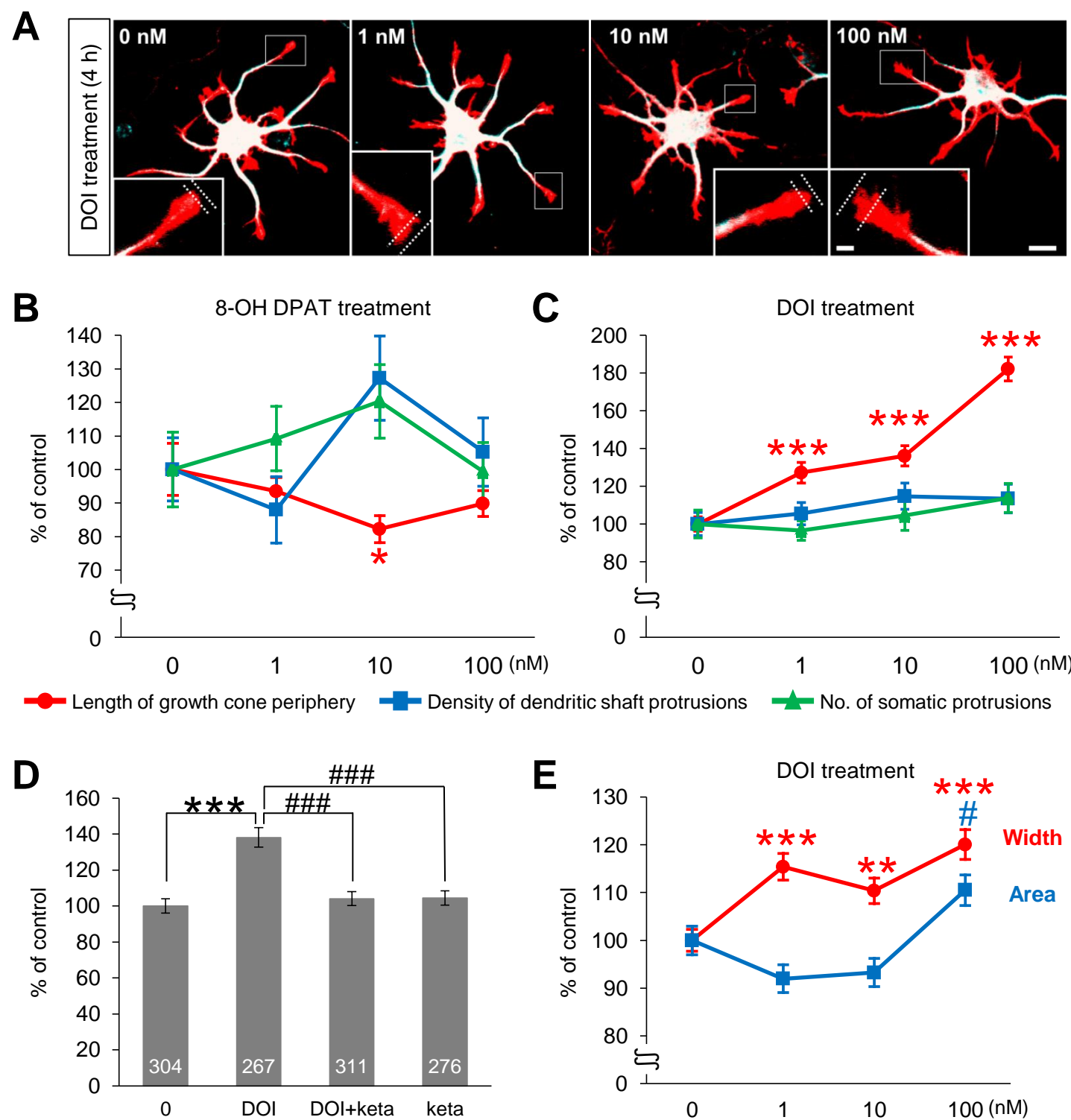


Figure 9. Effects of 8-OH DPAT and DOI on dendritic growth cone periphery and protrusions.

Cortical neurons were cultured for 4 days and treated with 8-OH DPAT and DOI for 4 hours. (A) Typical examples of neurons treated with DOI were shown. Growth cone periphery which was F-actin-positive and MAP2-negative were indicated between two dotted lines. (B, C) The length of growth cone periphery was decreased by 8-OH DPAT, whereas increased by DOI. Both agonists had no effects on the density of dendritic shaft protrusions and the number of somatic protrusions. (D) The DOI-induced increase of length of growth cone periphery was reversed by the concomitant treatment of ketanserin, 5-HT_{2A} receptor antagonist. (E) DOI also increased the width index and area of dendritic growth cone periphery. Scale bars: 5 μ m (A), 2 μ m (inset in A). Numbers in each bar shown in C indicate growth cone numbers. Data are shown as mean \pm SEM. * P < 0.05, ** P < 0.01, *** P < 0.001, # P < 0.05, ### P < 0.001

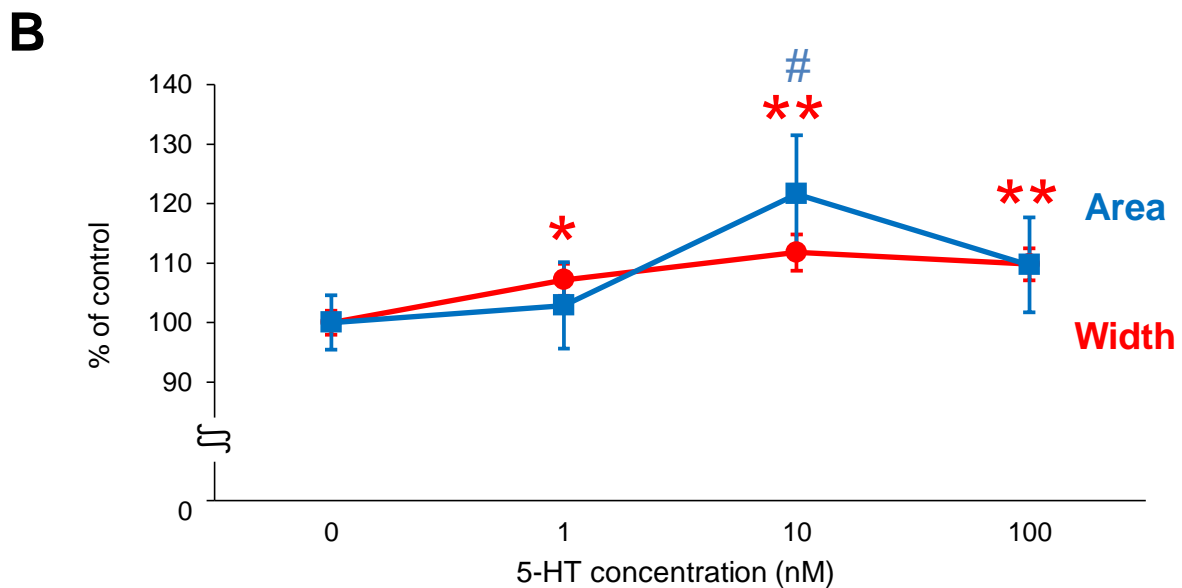
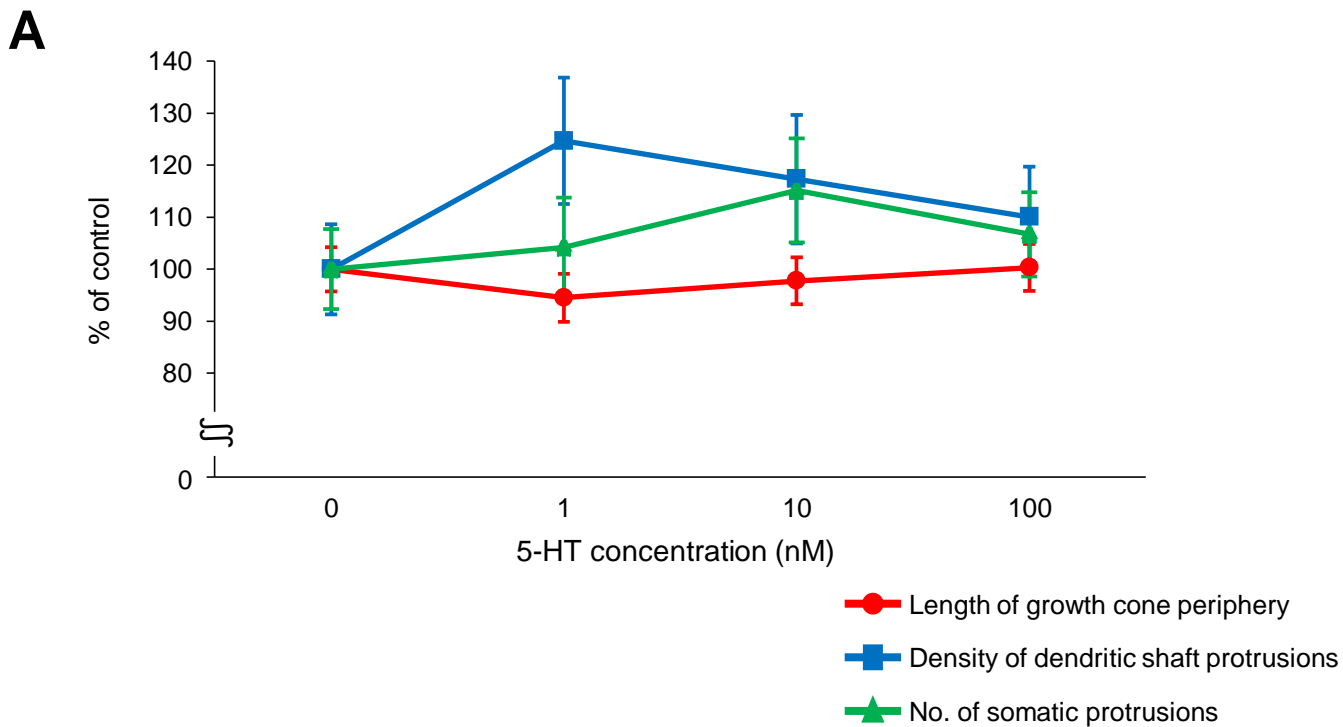


Figure 10. Effects of 5-HT on dendritic growth cone periphery and protrusions.

Cortical neurons were cultured for 4 days and treated with for 4 hours. 5-HT had no effect on the length of growth cone periphery, the density of dendritic shaft protrusions and the number of somatic protrusions (A), whereas increased the width index and area of growth cone periphery (B). Data are shown as mean \pm SEM. * $P < 0.05$, ** $P < 0.01$, # $P < 0.05$

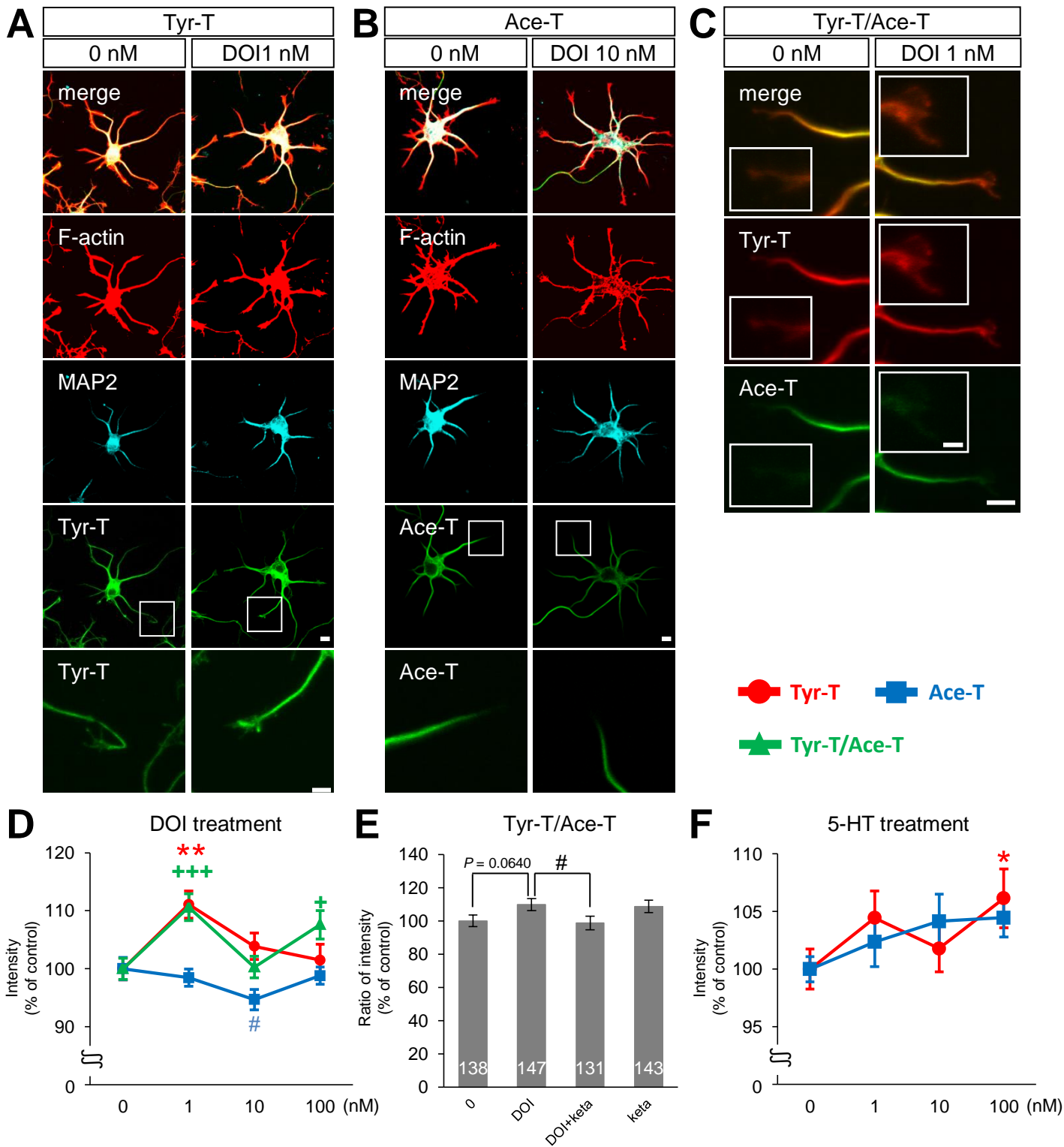


Figure 11. Effects of DOI and 5-HT on cytoskeletal proteins in dendritic growth cone periphery.

Cortical neurons were cultured for 4 days and treated with DOI or 5-HT for 4 hours. Neurons were stained for dynamic tubulin (Tyr-T) or stable tubulin (Ace-T) together with MAP2 and F-actin. (A, B) The fluorescence intensity of Tyr-T and Ace-T was measured in dendritic growth cone periphery. (C) The ratio of the intensity of Tyr-T and Ace-T (Tyr-T/Ace-T) was calculated in different growth cones from those shown in A and B. (D-F) The quantitative analysis of the fluorescence intensity of Tyr-T and Ace-T. (D) DOI increased the fluorescence intensity of Tyr-T (1 nM), whereas decreased the fluorescence intensity of Ace-T (10 nM). (D, E) The ratio of the intensity of Tyr-T/Ace-T was increased by 1 and 100 nM DOI in growth cones, and the effect of 1nM DOI was reversed by the concomitant treatment of 1000 nM ketanserin. Numbers in each bar indicate growth cone numbers. (F) The fluorescence intensity of Tyr-T was also increased by 100 nM 5-HT. Scale bars; 5 mm (A-C), 2 mm (insets in C). Data are shown as mean \pm SEM. * $P < 0.05$, ** $P < 0.01$, # $P < 0.05$, + $P < 0.05$, +++ $P < 0.001$

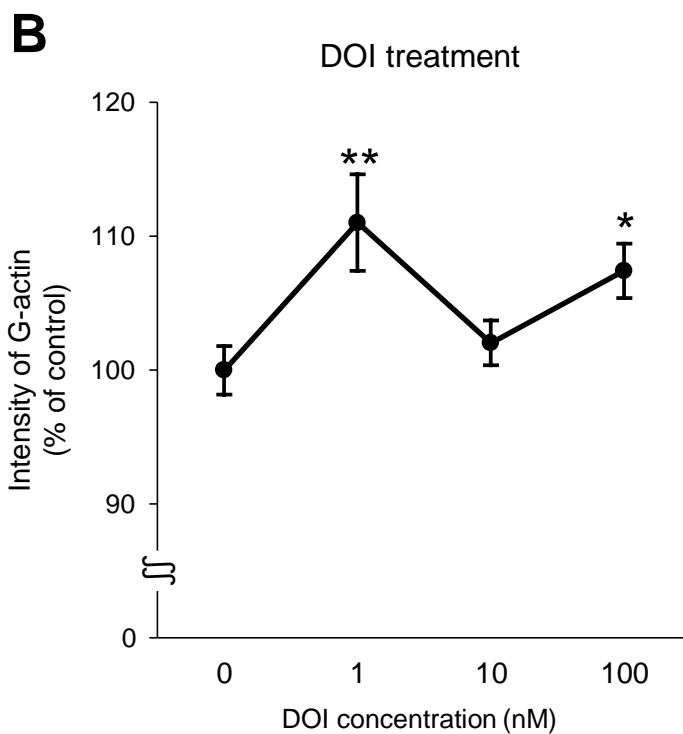
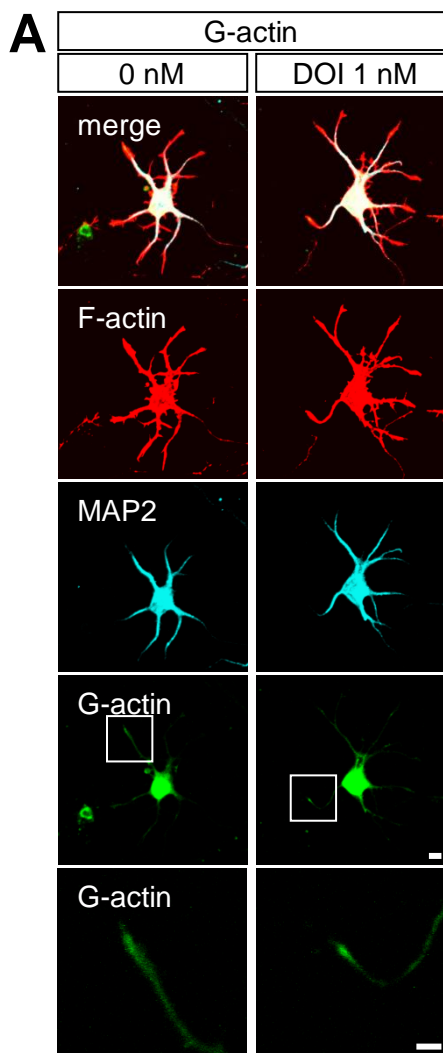


Figure 12. Effects of DOI on the expression of G-actin in dendritic growth cone periphery.

In cortical neurons treated with DOI for 4 hours, depolymerized actin (G-actin) was also measured in dendritic growth cone periphery. (A) Typical examples of neurons treated with DOI and stained for G-actin. (B) DOI increased the fluorescence intensity of G-actin (1 and 100 nM). Scale bars; 5 μ m (A). Data are shown as mean \pm SEM. * $P < 0.05$, ** $P < 0.01$

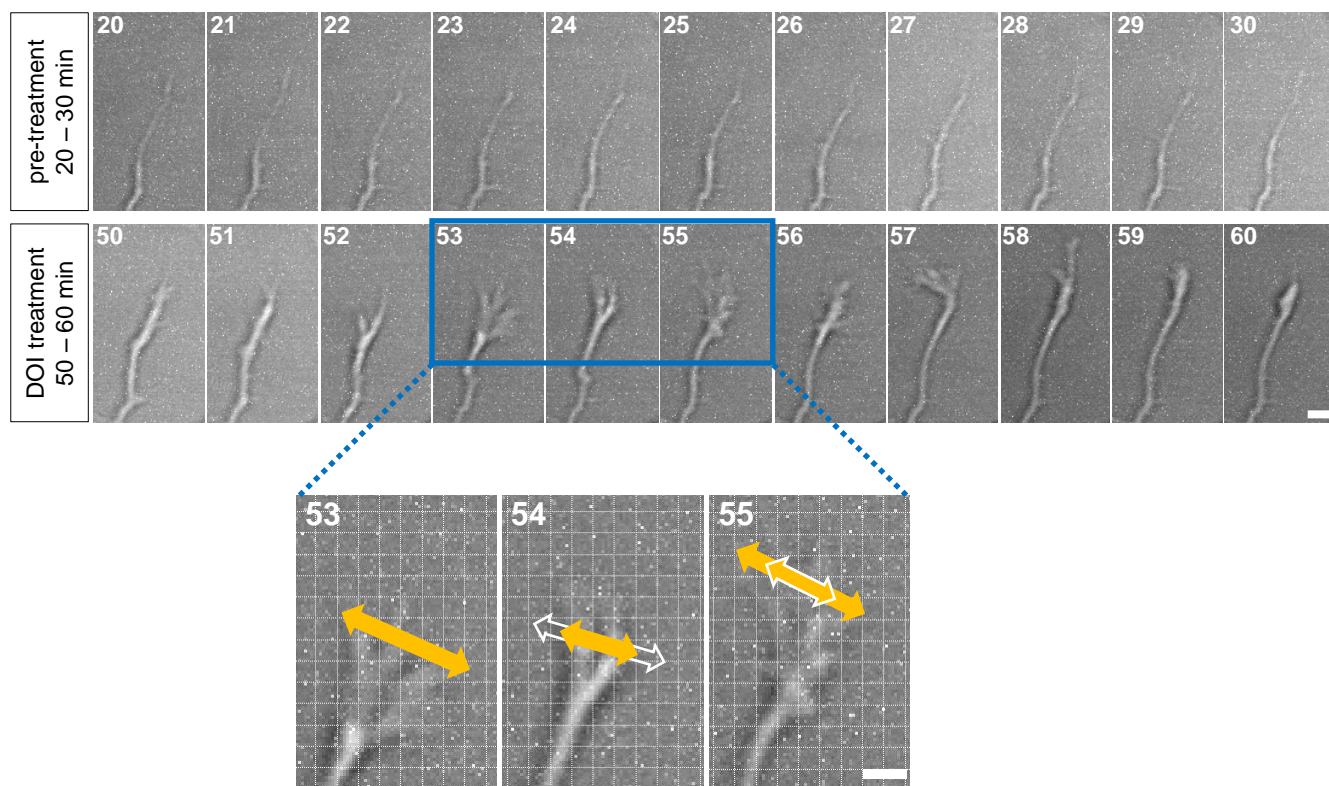
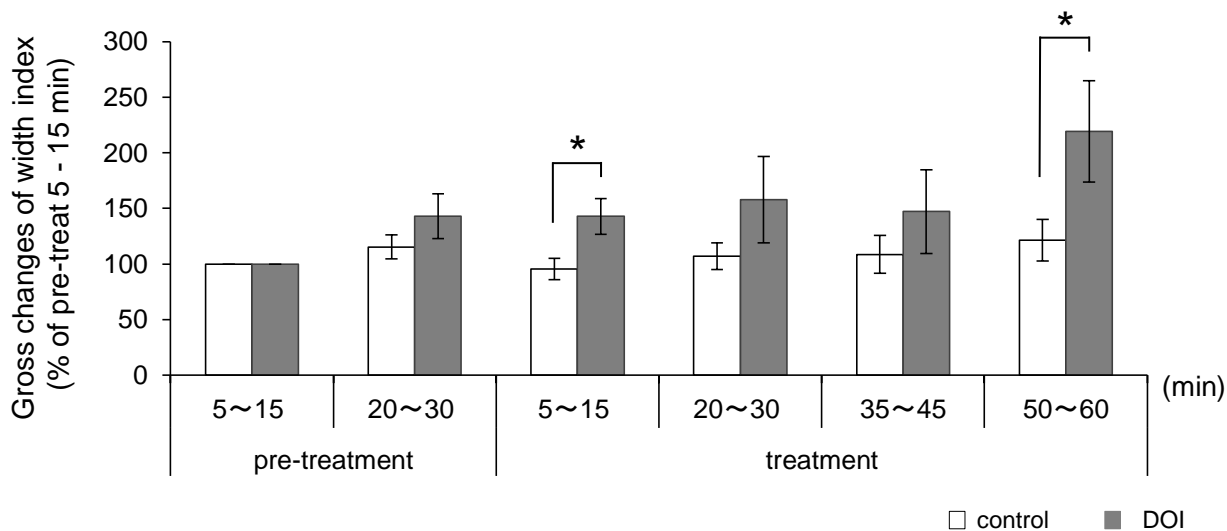
A**B**

Figure 13. Effects of DOI on the dynamics of the dendritic growth cone morphology.

Effects of DOI on the dynamics of the dendritic growth cone morphology were examined by the time lapse microscopy as shown in Fig. 5. (A) Representative DIC images of dendritic growth cones in the 20-30 minutes-interval in the pre-treatment period and 50-60 minutes-interval in the experimental period were shown. Magnified images showed the width (yellow arrows) of the growth cone at a given time and the width of the same growth cone 1 minute before (white arrows). Scale bar: 2 μm. (B) The gross changes of the width index (head width/neck width) of dendritic growth cones in each interval were compared with those in 5-15 minutes-interval of the pre-treatment period as 100%. 100 nM DOI increased the gross changes of the width index at 5-15 minutes- and 50-60 minutes-intervals in the treatment period as compared with the control in same intervals. 13 growth cones from 3 neurons and 14 growth cones from 4 neurons were analyzed in control and experimental groups, respectively. Data are shown as mean ± SEM. **P* < 0.05.

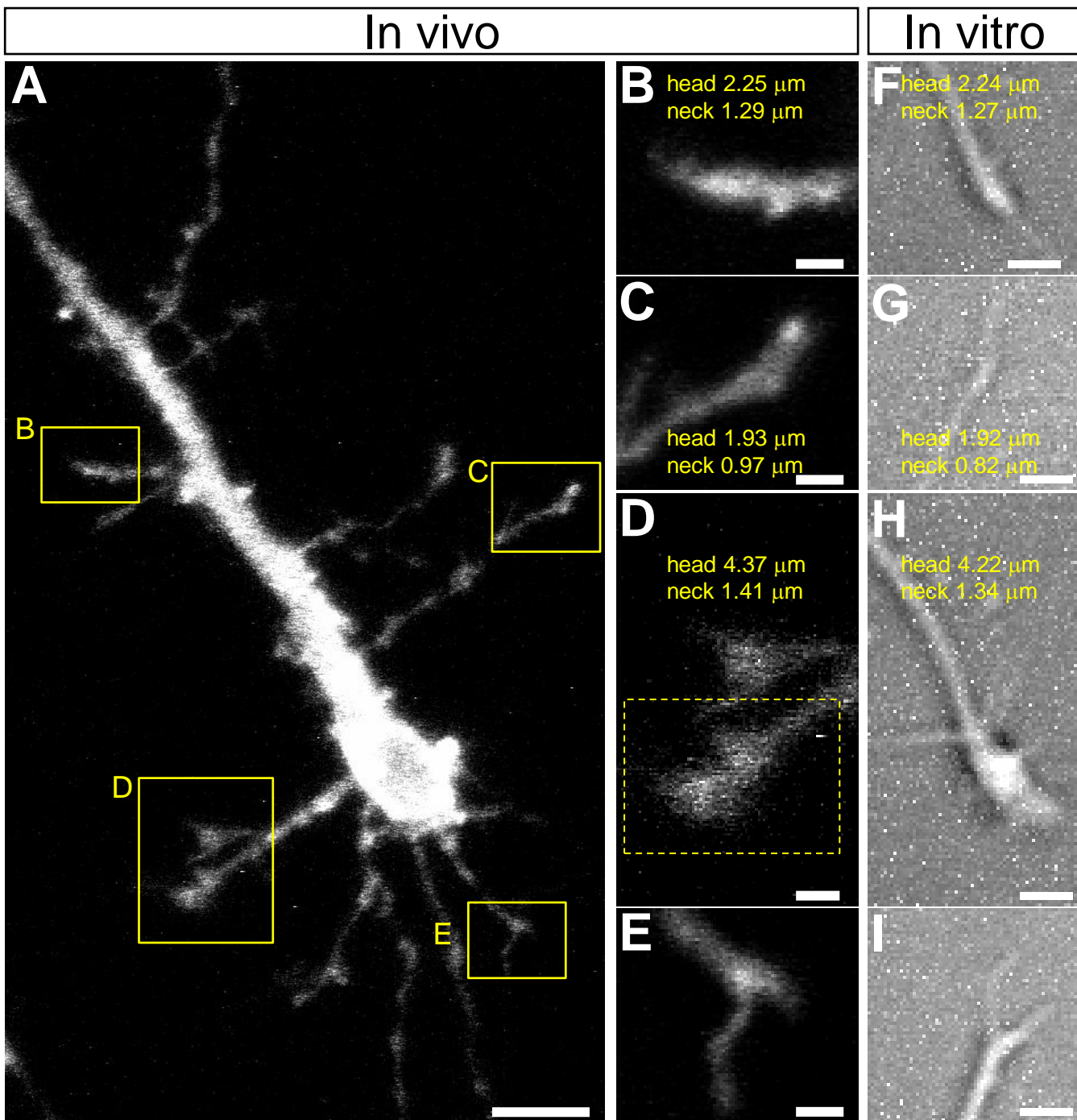


Figure 14. Dendritic growth cones of pyramidal neurons *in vivo*.

Neurons in the cerebral cortex at P0 were labeled by placing DiI crystals into the cerebral cortex. (A) Dendritic growth cones of pyramidal neurons had various morphologies. (B-E) are the magnified figures of yellow boxes in A. The head and neck width of these growth cones (except E) were measured, and growth cones *in vitro* were shown which were morphologically similar to each growth cone (F-I). Scale bar: 10 μm (A), 2 μm (B-I).